Impact of UV radiation on the Raman and infrared spectral signatures of sulfates, phosphates and carbonates: implications for Mars exploration

C. Royer, S. Bernard, O. Beyssac, E. Balan, O. Forni, Michel Gauthier, M. Morand, Y. Garino, P. Rosier

Impact of UV radiation on the Raman and infrared spectral signatures of sulfates, phosphates and carbonates: implications for Mars exploration

C. Royer[1,2], S. Bernard[3], O. Beyssac[3], E. Balan[3], O. Forni[4], M. Gauthier[3], M. Morand[3], Y. Garino[3] and P. Rosier[3]

[1]LESIA, Observatoire de Paris, Université PSL, CNRS, Sorbonne Université, Université de Paris, Meudon, France.
[2]Purdue University Earth, Atmospheric and Planetary Sciences department, West Lafayette, IN, USA
[3]Institut de Minéralogie, Physique des Matériaux et Cosmochimie, CNRS UMR 7590, Muséum National dHistoire Naturelle, Sorbonne Université ; Paris, France
[4]IRAP, CNRS, Université de Toulouse, UPS-OMP, Toulouse, France

Abstract: *Perseverance* is on Mars, collecting samples which will inform about Martian paleoenvironmental conditions. However, the surface of Mars is continuously bombarded by ionizing radiation, including UVs, which may significantly alter hydrated mineral phases such as sulfates, phosphates and carbonates. To explore and constrain this effect, we experimentally exposed pellets of more or less hydrated minerals to UV radiation within a Martian chamber at a temperature relevant for the rocks at the surface of Mars. Results show that exposure to UV leads to a strong alteration of the Raman and IR signals of sulfates, phosphates and carbonates. The strong increase of the luminescence signals coupled to the decrease of the Raman signals relatively to the background and the clear attenuation of the IR signals are interpreted as caused by an increasing concentration of electronic defects. The present results have strong implications for the ongoing exploration of Mars: one should not expect to detect pristine materials, except over freshly excavated surfaces. Still, as a precaution, all the targets measured or collected on Mars should be considered as having been exposed to UV radiation to some extent.

Highlights

- The surface of Mars is continuously bombarded by ionizing radiation, including UVs.
- Here we experimentally investigate the effect of UVs on spectral signals of minerals.
- Exposure to UVs alters Raman and IR signals of sulfates, phosphates and carbonates.
- Exposure to UVs clearly enhances the creation of electronic defects.
- Such effect has to be taken into account when interpreting data collected on Mars.

The *Perseverance* NASA rover is exploring the Jezero crater on Mars using an arsenal of spectroscopic tools to characterize the geological settings of the samples that will be returned to Earth (Farley et al., 2020; Maurice and Wiens, 2021; Wiens et al., 2021) by the NASA-ESA Mars Sample Return program (Meyer et al., 2022). Although the surface of Mars is globally cold and dry today, environments with liquid water likely existed during the Noachian (Grotzinger et al., 2014; McMahon et al., 2018; Farley et al., 2020). A number of minerals, such as many of those belonging to the phyllosilicate, sulfate, or carbonate groups, may have been produced via aqueous alteration processes having occurred at the surface and potentially carry invaluable information about the climatic conditions

that prevailed on Mars during the Noachian (Vaniman et al., 2004; Bibring et al., 2005; Poulet et al., 2005; Mustard et al., 2008; Murchie et al., 2009; Carter et al., 2010). Alternatively, other minerals like phosphates, which may crystallize during magmatic processes, may provide crucial information on the volatile content of the deep planet. Their identification and the determination of their water content may thus shed new light on the early geologic and climatic history of Mars.

Although infrared (IR) spectroscopy has long been used from orbit only with CRISM or OMEGA to identify minerals on Mars (Bibring et al., 2005; Poulet et al., 2005; Mustard et al., 2008; Murchie et al., 2009; Carter et al., 2010; Ehlmann et al., 2011), IR data can now be collected from the ground using the SuperCam instrument aboard *Perseverance* (Maurice and Wiens, 2021; Wiens et al., 2021; Fouchet et al., 2022). Furthermore, IR data can be directly confronted to Raman spectroscopic data collected using SuperCam (Wiens et al., 2022; Clavé et al., 2023; Beyssac et al., 2023) or SHERLOC (Bhartia et al., 2021; Scheller et al., 2022a). A similar strategy, *i.e.*, allowing both IR and Raman data to be collected on the same targets, has been adopted by ESA for Rosalind Franklin, the rover of the ExoMars mission, which will be equipped with two IR instruments (ISEM Korablev et al. 2017 and MicrOmega Bibring et al. 2017), and one Raman instrument (RLS Rull et al. 2017). The combined use of IR and Raman spectroscopies at the surface of Mars is expected to allow identification of minerals and quantification of their water content.

However, as is the case for organic molecules at the surface of Mars (Fornaro et al., 2018; Fox et al., 2019; Megevand et al., 2021), these minerals have been bombarded by ionizing radiation. In fact, in the absence of a global magnetic field, the thin CO_2 atmosphere of Mars absorbs most X-rays and far-UV radiation, but lets mid- and near-UV photons in the range 190 – 410 nm, gamma rays, solar energetic protons, and galactic cosmic rays reach the surface (Patel et al., 2002; Dartnell et al., 2007; Hassler et al., 2014). Even though UV photons do not penetrate that much below the surface (Carrier et al., 2019), they can interact with minerals exposed at the surface, altering their composition via radiolysis and their structure via the incorporation of electronic defects. Such alteration may modify their spectral responses for techniques sensitive to the crystal structure, chemical nature and hydration signature (H_2O and OH), such as Raman and infrared spectroscopies (Dartnell et al., 2007; Hassler et al., 2014). This may lead to misinterpretations of the collected signals. Worse, most mineral calibration targets having served to characterize instrumental responses are terrestrial analogues which have never experienced the levels of UV radiation bombarding the surface of Mars (Manrique et al.,

2020). Experimentally constraining in the laboratory the impact of UV radiation on the structure, water content and spectral signatures of hydrated and non-hydrated minerals is therefore critical to properly interpret the data collected on Mars.

The evolution of the IR spectral signatures of sulfates, phosphates or carbonates experimentally exposed to simulated Mars surface UV radiation conditions has been investigated by a rather limited number of authors (Bish et al., 2003; Cloutis et al., 2007, 2008; Poitras et al., 2018; Turenne et al., 2022). An even lower number of studies have been dedicated to the evolution of their Raman spectral signatures (Bonales et al., 2022). Of note, extrapolating laboratory results to natural settings remains difficult, in particular because geological timescales cannot be replicated in the laboratory, questioning the intrinsic relevance of laboratory experiments. Yet, the instruments onboard *Perseverance* do not only measure rocks having been exposed to UV radiation for millions or billions of years. In fact, *Perseverance* carries an abrasion tool allowing the exposure of a patch of 5 cm diameter of pristine rock initially lying 2 to 16 mm below the surface (Moeller et al., 2020), to be studied using spectroscopic tools within a few Martian Sols. This justifies experimental investigations, even over short timescales. Following a previous study dedicated to the impact of UV radiation on organic molecules (Megevand et al., 2021), we have therefore conducted laboratory experiments to document the impact of UV radiation on the water content and structure of mineral phases of major interest in the current exploration of Mars.

Here, we first investigated the evolution of the Raman and IR spectroscopic signatures of initially more or less hydrated sulfates (Ca, Na, Mg, Fe, and Al-rich sulfates) during an experimental exposure to UV radiation within a Martian chamber at a temperature relevant for the rocks at the surface of Mars. Sulfates are of particular interest in the context of the Mars2020 mission as they are considered as having a high biopreservation potential (Scheller et al., 2022b), and they may also result from the interaction of water with rocks. We also conducted similar experiments for a slightly longer duration using phosphates (Ca, Na and Mg-rich phosphates) and carbonates (Ca, Na and Mg-rich carbonates) since these minerals are also of high interest for astrobiology (McMahon et al., 2018) and more generally for geology. The Raman spectra of these minerals were collected during the experiments *in situ* within the Martian chamber, while their IR spectra were collected at the end of experiments, once the irradiated samples were removed from the Martian chamber.

1 Materials and Methods

1.1 Selected minerals and general strategy

Five sulfates (exhibiting different hydration states), three phosphates (exhibiting different hydration states) and three carbonates (exhibiting different hydration and hydroxylation states) were selected for the present study (cf Table 1). Besides for the hydromagnesite (*i.e.*, the Mg-rich hydrocarbonate for which a natural single crystal was simply taped on a Scanning Electron Microscope stub), we used a mechanical press to prepare pellets of compressed samples (several mg of each mineral were pressed at 2 tons onto a stub of 1 cm in diameter, leading to a final thickness of about 1 mm). Irradiation experiments were conducted in a dedicated Martian chamber built by the Cellule Projet @ IMPMC (Fig. 1) (Megevand et al., 2021). In this chamber, samples are exposed to UV radiation at 0°C under a primary vacuum ($<$ 1 mbar). A Martian-like CO_2 atmosphere was not introduced into the chamber to prevent absorption of UV by CO_2 and contamination from air. Previous studies have shown that a few mbars of CO_2 have no influence on the UV induced degradation of amino acids (ten Kate et al., 2006), nor on the UV induced dehydration of sulfates (Bonales et al., 2022). Of note, all the samples have been introduced into the Martian chamber and exposed to the pressure and temperature conditions of the experiments for 15 hours before being exposed to UV radiation. Such exposition to low pressure and temperature conditions did not have any effect on the degree of hydration of the samples investigated here as verified using Raman spectroscopy directly performed in the chamber. Samples were then exposed to UV produced by a 150 W arc lamp equipped with a high pressure Xenon bulb (UXL-150SP - LOT-ORIEL). Note that this is the exact same lamp which the Mars Organic Molecule Irradiation and Evolution (MOMIE) setup relies on (Stalport et al., 2009, 2019; Poch et al., 2013, 2014) and which was used to document the impact of UV radiation on cystine (Megevand et al., 2021). This lamp delivers a UV spectrum (190 – 400 nm) with a pattern similar to that of the Martian surface radiation spectrum (Patel et al., 2002; Dartnell et al., 2007; Hassler et al., 2014), and a flux of the same order of magnitude as the one undergone by the Martian surface, simulating well true Martian conditions. Note that a DUV Grade Fused Silica window allowed rejecting most of the IR radiation (down to 2.89 µm), mitigating a potential heating of the samples by the UV lamp although the 400 nm – 2.89 µm range is still available for radiant heating (Fig. 2). Raman spectra of starting and irradiated materials were measured directly in the Martian chamber (from 200 to 2000 cm^{-1} and

from 3000 to 4000 cm^{-1}), that is, under the conditions of the experiments. The Raman spectra of sulfate samples were measured before and after 30 and 270 min of exposure to UV radiation, while those of phosphate and carbonate samples were measured before and after 5, 30, 270 and 1500 min of exposure to UV. At the end of the irradiation experiments (*i.e.*, after 270 minutes for sulfates and after 1500 minutes for phosphates and carbonates), samples were removed from the chamber and measured with diffuse reflectance IR spectroscopy (over the 1–2.75 µm range). Note that the contribution of the volume of irradiated materials to the measured signals differed from one technique to another as the total volume probed is different for Raman and IR spectroscopies (and rather difficult to estimate), challenging the direct comparison between the data.

Name	Formula	Ref. Sigma-Aldrich/N°CAS
Calcium sulfate dihydrate	$CaSO_4 \cdot 2\,H_2O$	1.02161/10101-41-4
Sodium sulfate	Na_2SO_4	239313/7757-82-6
Aluminum sulfate, octadecahydrate	$Al_2(SO_4)_3 \cdot 18\,H_2O$	227617/7784-31-8
Magnesium sulfate	$MgSO_4$	M7506/7487-88-9
Iron sulfate (III), hydrate	$Fe_2(SO_4)_3 \cdot x\,H_2O$	307718/15244-10-7
Calcium phosphate	$Ca_3(PO_4)_2$	21218/7758-87-4
Sodium phosphate	Na_3PO_4	342483/7601-54-9
Magnesium phosphate hydrate	$Mg_3(PO_4)_2 \cdot x\,H_2O$	344702/53408-95-0
Calcium carbonate	$CaCO_3$	10679-36/471-34-1
Sodium carbonate, decahydrate	$Na_2CO_3 \cdot 10\,H_2O$	1.06391/6132-02-1
Hydromagnesite	$4\,(MgCO_3)Mg(OH)_2 \cdot 4\,H_2O$	*Natural sample*

Table 1: List of the studied samples.

1.2 Time resolved Raman and IR reflectance

Following Fau et al. (2019, 2022) and Megevand et al. (2021), we relied on a customized time-resolved Raman spectrometer built by the Cellule Projet at IMPMC to collect the Raman spectra of the samples investigated. Within the Martian chamber used here, samples are at a distance of 8 meters from the telescope, mimicking the configuration of remote Raman measurements conducted on Mars using SuperCam. Here, the fine control and synchronization of both time delay and gating time of the camera allows sub-nanosecond time resolution experiments: we collected Raman signals using a 2 ns ICCD gate centered on the 1.2 ns laser pulse. Filters are used to limit the laser irradiance at the surface of samples below 10^{10} W/m^2 to prevent any laser-induced damage (Fau et al., 2019). In the remote setting, the laser is collimated at the sample surface 8 m from the telescope Schmidt plate on a spot of

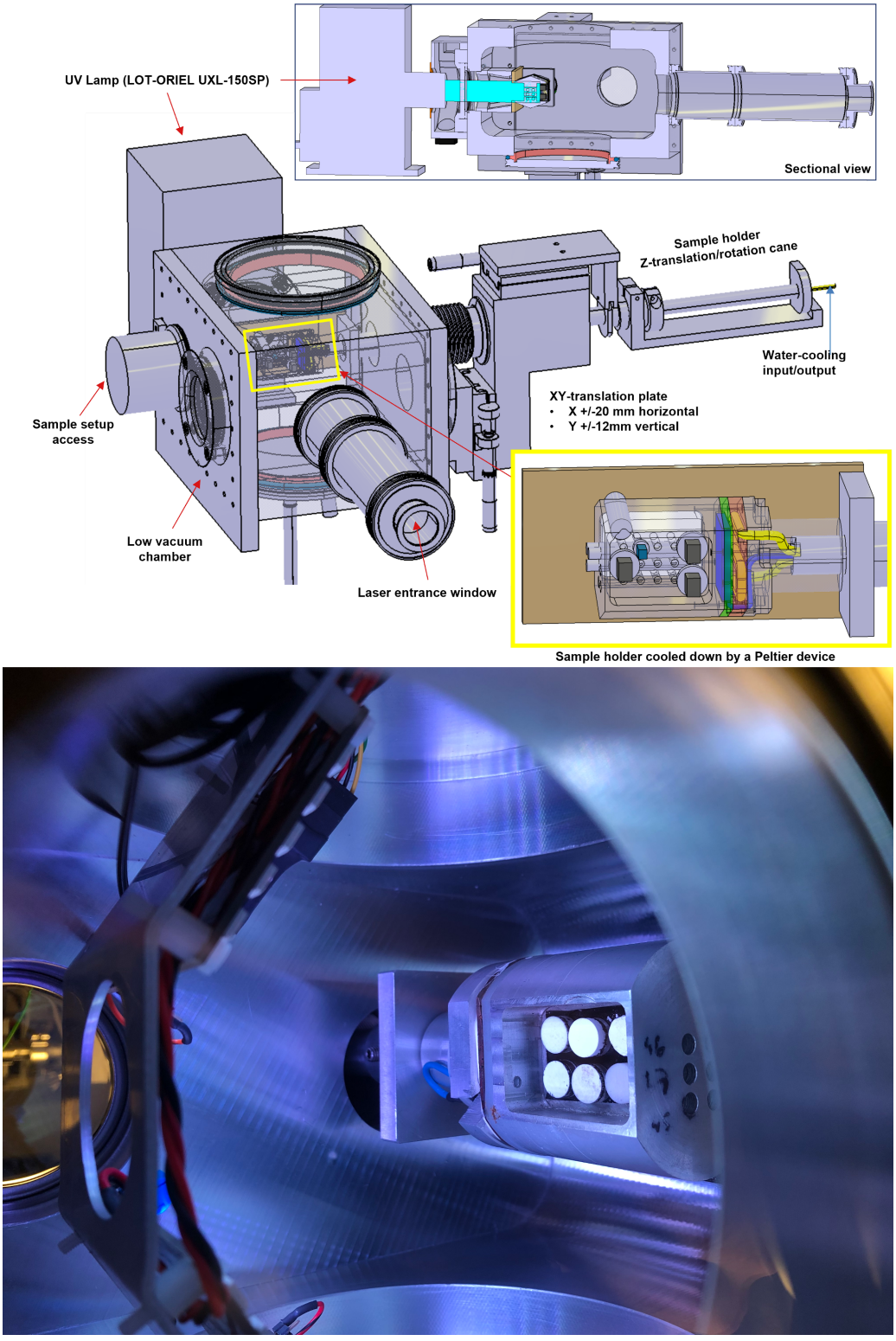

Figure 1: Top: CAD images of the chamber, its illumination device and the sample holder mechanism. Bottom: Picture of the vacuum chamber containing the samples (the 6 cylindrical pellets) seen from the Raman measurement side. The plate can translate in two degrees of freedom to center each pellet in the laser beam. The pierced plate in the foreground contains an illumination system to facilitate the positioning of the pellets.

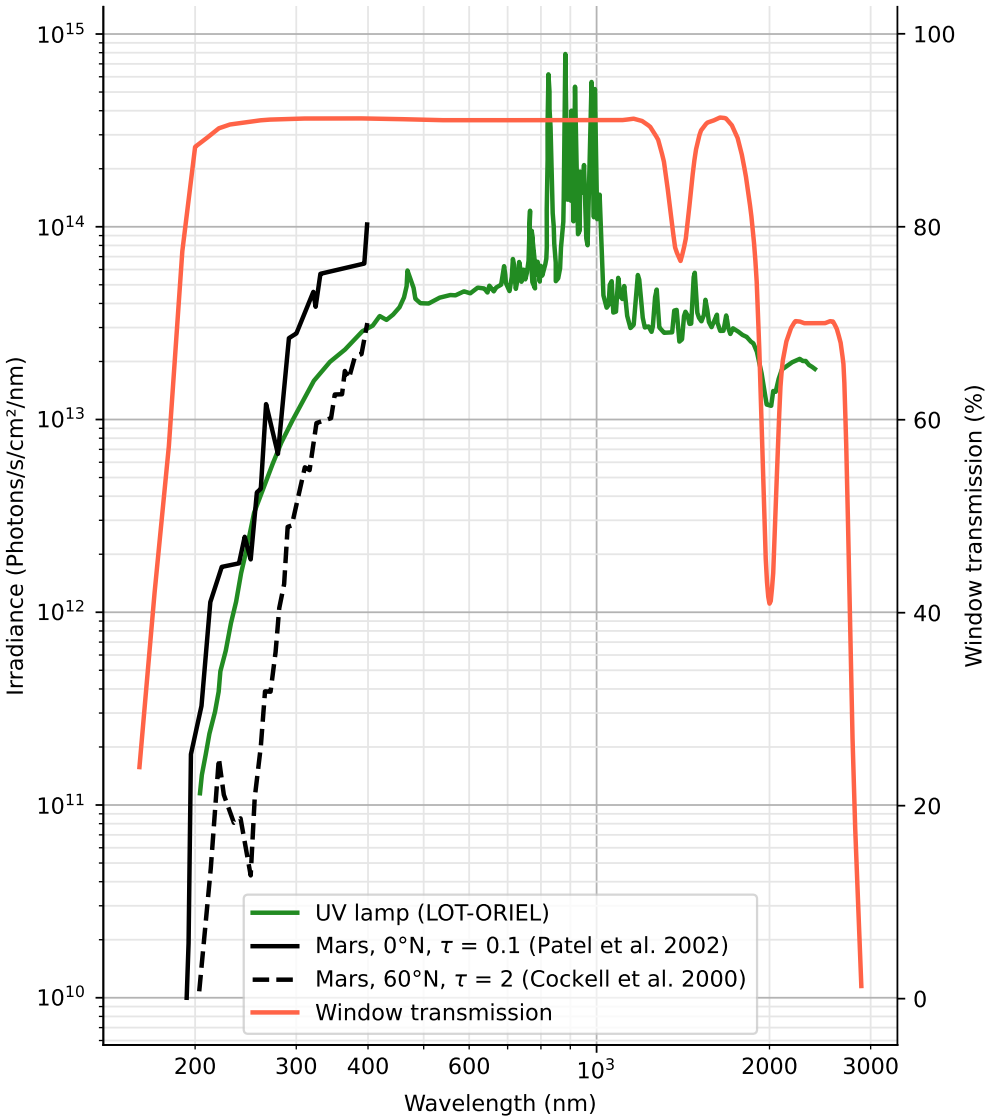

Figure 2: Irradiance spectra of the lamp (green line) compared to the sun at the Martian equator and under clear atmosphere (solid black line) and at N 60° latitude under more opaque atmosphere (dashed line), in the UV range; transmission spectrum of the fused silica window (red line).

$\sim$ 6 mm diameter, and the Raman signal is collected by a conventional Schmidt-Cassegrain telescope (Celestron-C8 202 mm diameter Schmidt plate) on a spot of $\sim$ 5 mm diameter co-aligned with the laser spot. After the telescope, a notch filter cuts off the Rayleigh scattering at $\sim$ 90 cm^{-1} and the signal is collected by an optical fiber and sent into the modified Czerny-Turner spectrometer coupled with the intensified ICCD camera. This spectrometer has three motorized gratings that can be selected depending on the spectral window and spectral resolution requested. Here, we used a 600 gr/mm grating yielding a spectral resolution of about 10–12 cm^{-1}, *i.e.*, spectral resolution similar to that

of the SuperCam instrument. To maximize the signal-to-noise ratio (SNR), we accumulated signals collected over 10^6 laser shots. We also collected the luminescence signal with no Raman contribution using a 100 µs ICCD gate opened just after the laser pulse (Fau et al., 2019, 2022; Megevand et al., 2021).

IR reflectance data were collected with a commercial Fourier transform spectrometer Nicolet 6700 FTIR operating at IMPMC over the 1 to 2.7 µm spectral range with a spectral resolution of 1 cm^{-1}, allowing for the detection of features related to hydration (H_2O vibrations) and structure (CO_3^{2-} and SO_4^{2-}). The acquired spectra were divided by a blank (a silver mirror) before any further processing. After being removed from the Martian chamber and prior to IR analysis, samples were conserved in a dry environment at low temperature in a cold room.

2 Results

2.1 Starting materials

The Raman and IR spectra of sulfates, phosphates and carbonates are extensively described in the literature (cf for instance Wang et al. 2006; Buzgar et al. 2009; Ben Mabrouk et al. 2013 for sulfates, Fau et al. 2022 for phosphates, and Gunasekaran et al. 2006; Harner and Gilmore 2015 for carbonates). For all these minerals, the most intense Raman peak is due to the ν_1 symmetric stretching mode of SO_4, PO_4 and CO_3 and located at $\sim$ 1010 cm^{-1}, $\sim$ 960 cm^{-1} and $\sim$ 1085 cm^{-1} for sulfates, phosphates and carbonates respectively. Additional peaks due to these molecular groups are the doubly degenerate ν_2 bending mode at $\sim$ 450 cm^{-1} and $\sim$ 430 cm^{-1} for sulfates and phosphates respectively (the ν_2 vibration peak is not observed in our carbonate samples), the triply degenerate antisymmetric ν_3 stretching mode at $\sim$ 1160 cm^{-1}, $\sim$ 1060 cm^{-1} and $\sim$ 1470 cm^{-1}, and the triply degenerate ν_4 bending mode at $\sim$ 640 cm^{-1}, $\sim$ 580 cm^{-1} and $\sim$ 720 cm^{-1}, always for sulfates, phosphates and carbonates respectively. Last, some lattice modes may be detected in these phases at lower wavenumbers. When present, H_2O contributes a broad band at $\sim$ 3400–3600 cm^{-1}, while HO^- contributes one or several sharp bands in the range $\sim$ 3500-3700 cm^{-1} (Fig. 3a, b, c).

The near infrared spectra of these materials show numerous absorption bands attributed to different overtones of the stretching (ν_1 and ν_3) and bending (ν_2 and ν_4) vibrations of the structural anion (SO_4^{2-}, CO_3^{2-} or PO_4^{3-}) combined with the vibrations of water present in the crystal or adsorbed

on its surface. In sulfates, we find similar spectra with absorptions at 1.2, 1.5 (triply degenerate in particular in $CaSO_4 \cdot 2\,H_2O$), 1.75, 1.92 and 2.25 μm. The carbonate samples show a wider range of spectra, with the main absorption bands related to structural water in Na_2CO_3 and to CO_3 in $CaCO_3$ (at 2.34 and 2.53 μm). Hydromagnesite shows in addition an absorption band around 1.4 μm assigned to the first overtone of the OH stretch and around 1.9 μm corresponding to the combination of stretching and bending of H_2O. Finally the phosphates present few spectral signatures in the infrared, except a band at about 1.9 μm related to the stretching and bending vibrations of water (Fig. 3d, e, f).

2.2 Evolution of sulfates with increasing irradiation

2.2.1 Luminescence

The luminescence signal (collected using a 100 μs ICCD gate opened just after the laser pulse) strongly increases with increasing irradiation duration (Fig. 4). The increase of this luminescence roughly follows a first-order logarithmic law with time (Fig. 4f), highlighting that UV radiation has had the most impact at the beginning of the experiments. This luminescence seems to have a short lifetime, since most of it is not rejected even when using a 2 ns ICCD gate centered on the 1.2 ns laser pulse to collect the signal. Because of this strong luminescence contribution, the Raman spectra collected in the present study have all been normalized to the total signal received by the spectrometer, to discuss the evolution of the Raman signal relative to the background contribution (Fig. 5).

2.2.2 Raman signal

The Raman signal of sulfates (*i.e.*, the Raman peaks of the signal collected using a 2 ns ICCD gate centered on the 1.2 ns laser pulse) decreases with increasing irradiation duration relative to the background contribution as shown when data are normalized to the total signal received by the spectrometer (Fig. 5). Irradiation seems to be responsible for a modification of the background shape (*i.e.*, the slope of the background has increased with increasing irradiation duration). After 270 minutes of irradiation, only the main ν_1 peak can still be observed. No new peak is observed in any of the spectra of the irradiated sulfates. After removal of the background, peaks were fitted using Lorentzian functions which areas were normalized to those of the functions used to fit the peaks of the starting materials. This parameter decreases exponentially as a function of the duration of irradiation

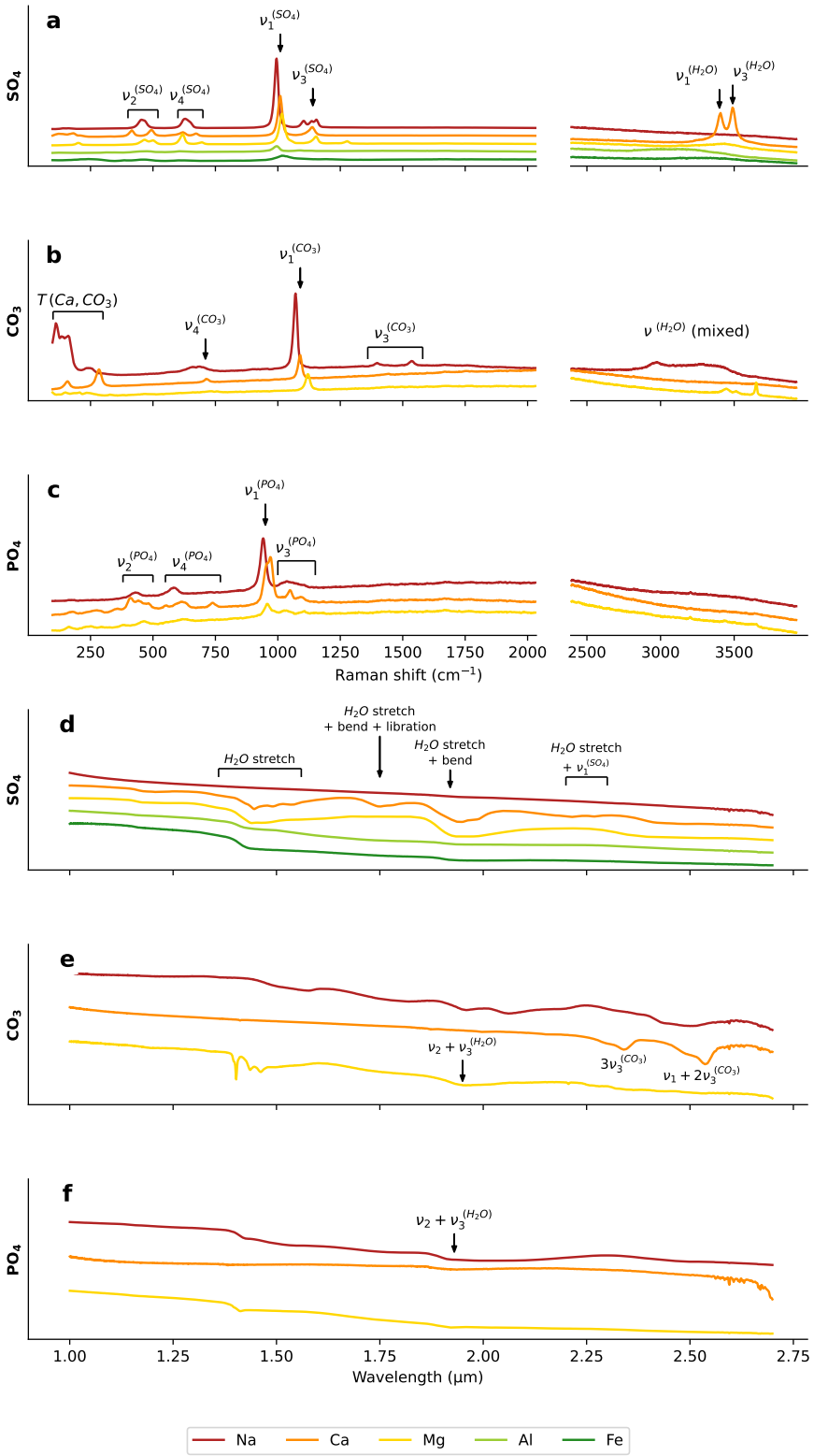

Figure 3: Raman (a, b, c) and IR (d, e, f) spectra of the studied minerals before irradiation, normalized and shifted for clarity. The attribution of their main features is indicated. More details about the attribution of the sulfates near-IR absorption features are given in Supplementary materials.

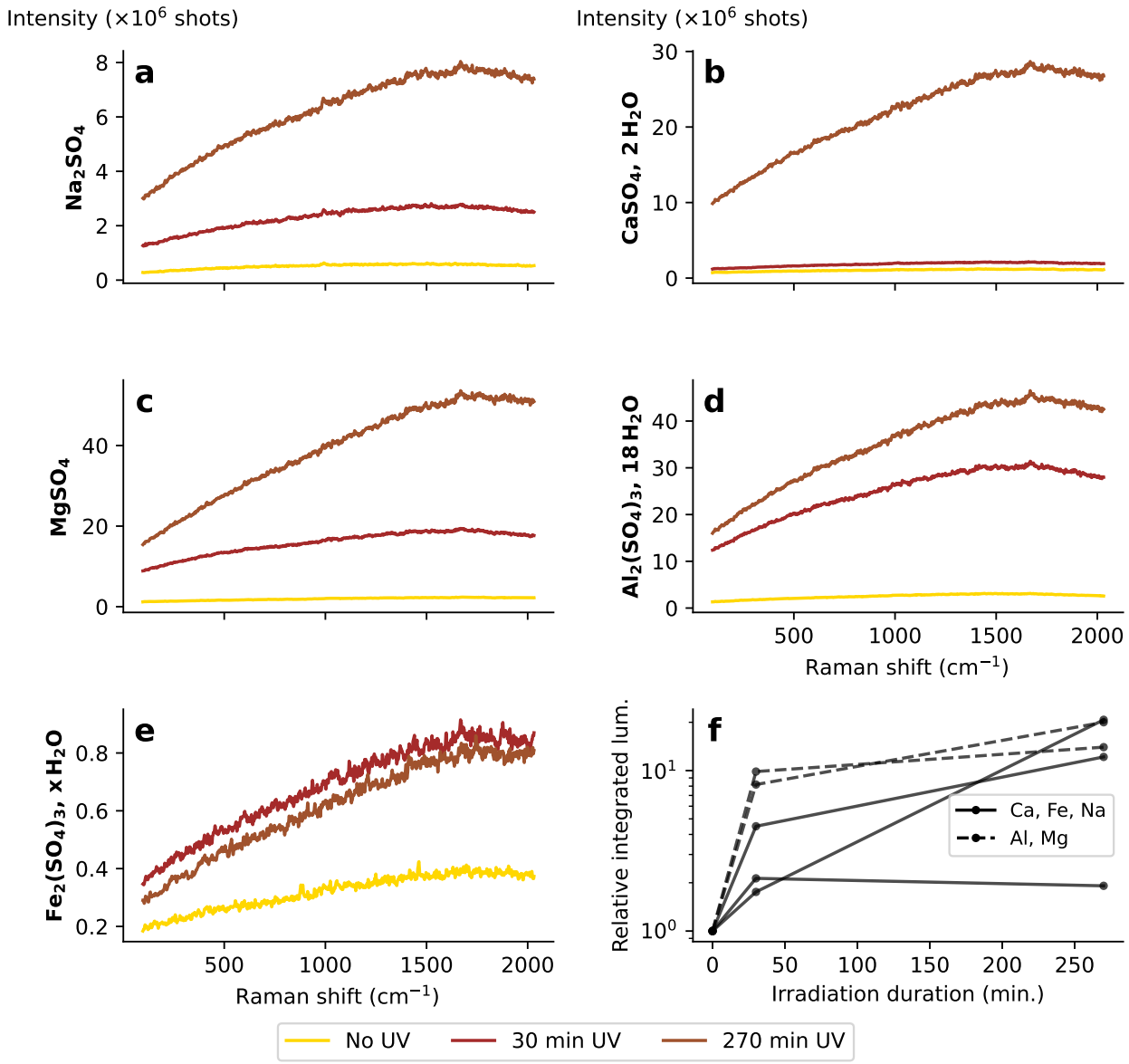

Figure 4: **a** to **e**: Raw luminescence spectra of sulfate samples as a function of irradiation duration. **f**: Relative total integrated luminescence as a function of the irradiation duration for each sulfate sample.

(Fig. 5f), highlighting, as for the luminescence, that the impact of UV radiation was maximum at the beginning of the experiments.

2.2.3 Raman-based water detection

The specific sub-peak structures in their Raman water bands at about 3400 cm^{-1} provide direct information on the hydration states of sulfates (Wang et al., 2006). The sulfates selected for the present experiments initially exhibit different hydration states, from anhydrous ($Na_2SO_4 \cdot 0\,H_2O$) to

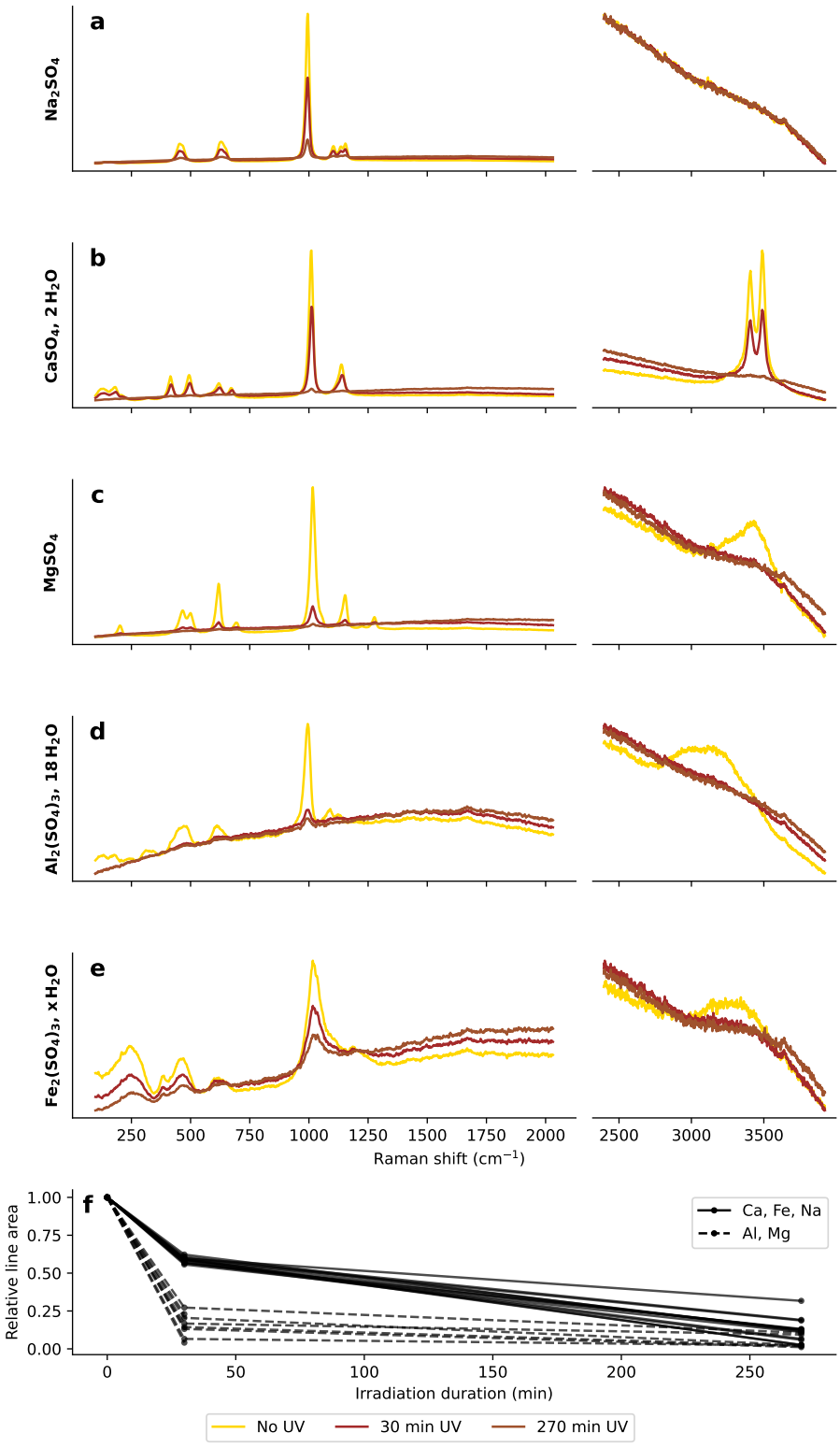

Figure 5: **a** to **e**: Raman spectra of the various sulfate minerals measured with a 2 ns gate. The spectra have been normalized by their total surface to highlight their relative variation. **f**: relative area of each major Raman scattering line as a function of the irradiation duration.

highly hydrated ($Al_2SO_4 \cdot 18\,H_2O$). Besides for the Na-rich sulfate, the exposure of sulfates to UV irradiation appears to be responsible for the disappearance of the peaks related to the structural water they initially contain. In fact, with the exception of the Ca-rich sulfate, all the initially hydrated sulfates investigated do not anymore show Raman hydration feature at about 3400 cm^{-1} (Fig. 5). This is also the case for the Ca-rich sulfate after 270 minutes of irradiation.

2.2.4 IR signal

At the end of the irradiation experiments (*i.e.*, after 270 minutes of exposure to UV), the sulfates investigated were measured with IR spectroscopy and their spectra were compared to those of the starting materials (Fig. 6). The absorption bands corresponding to the stretching/bending vibrations of the H_2O and OH groups, to various combinations of these modes and to overtones with SO_4 modes (*e.g.*, at 2.217 and 2.268 µm in gypsum), can still be observed in the near-IR reflectance spectra of the sulfates having been exposed to UV radiation for 270 minutes. The observed enlargement of the absorption bands after exposure to UVs indicate the creation of electronic defects rather than dehydration. Of note, atmospheric water may have been adsorbed onto the samples during their storage at 0°C before NIR measurements despite the presence of a desiccant.

2.3 Evolution of phosphates and carbonates with increasing irradiation

The phosphates and carbonates investigated here were exposed to UV radiation conditions similar to those to which sulfates were exposed, but for a slightly longer duration. The luminescence and Raman signals of the phosphates and carbonates were collected after 5, 30, 270 and 1500 min of exposure to UV and compared to the spectra of the starting materials (Figs. 7 - 8). As observed for sulfates, the luminescence signals of phosphates and carbonates strongly increase with increasing irradiation duration, and their Raman signals decrease with increasing irradiation duration relative to the background contribution. Note that, as for sulfates, the Raman spectra of phosphates and carbonates have all been normalized to the total signal received by the spectrometer. Irradiation seems to be also responsible for a modification of the background shape (*i.e.*, the slope of the background has increased with increasing irradiation duration). After 1500 minutes of irradiation, only the main peaks of phosphates and carbonates can still be observed (*i.e.*, the ν_1 peaks at about 960 cm^{-1} and 1085 cm^{-1}, of ${PO_4}^{3-}$ and ${CO_3}^{2-}$, respectively). No new peak is observed in any of the spectra of the

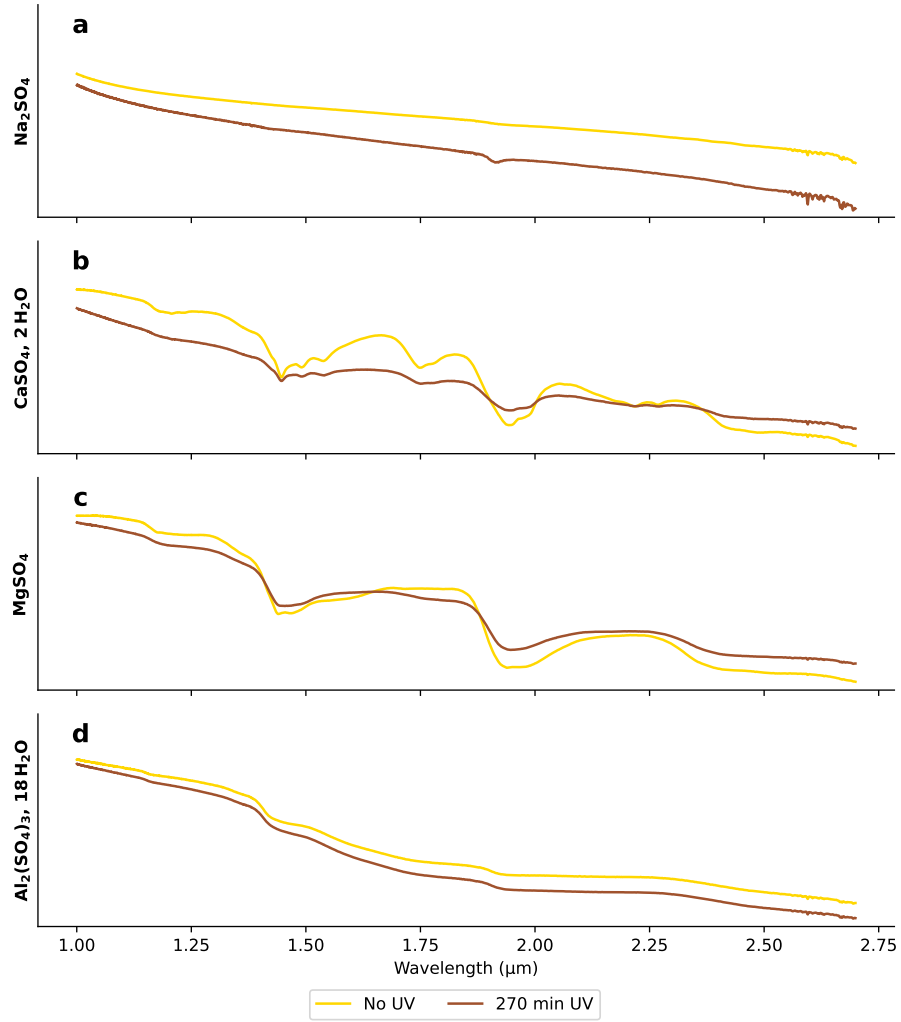

Figure 6: Near-infrared spectra of sodium sulfate (**a**), calcium sulfate (**b**), magnesium sulfate (**c**) and aluminum sulfate (**d**).

irradiated phosphates and carbonates. As for sulfates, results of peak fitting reveal that the decrease of the Raman signal decreases exponentially as a function of the duration of irradiation (Figs. 7d – 8d), highlighting, as the luminescence is exponential, that UV radiation has had the most impact at the beginning of the experiments.

Of note, the Raman signal of phosphates evolves a bit faster with experiment duration (peak decrease and background increase) than that of carbonates, suggesting a priori that phosphates are less resistant to UV than carbonates. But this may be related to the ratio of the volume effectively probed by Raman to the volume effectively affected by UV radiation. A higher contribution to the signal of a pristine volume of sample (*i.e.*, a volume unaffected by UV) would artifactually indicate a higher resistance to UV. For instance. the hydromagnesite seems to be the most UV-resistant sample

of all the samples investigated here, but it is also the only transparent monocrystal investigated (all the other samples were pressed into pellets). For instance, the volume of pristine hydromagnesite *in fine* contributing to the Raman spectra collected on this target may thus be a lot larger than the volumes of the pristine parts of the other samples contributing to the measured signals, thereby artifactually minimizing the effect of exposure to UV on the Raman signal. Most of the phosphates investigated here were nominally anhydrous, except for the magnesium phosphate, and thus exhibited no Raman water bands at about 3400 cm^{-1} and 3600 – 3700 cm^{-1} for OH in hydromagnesite. Still, the negative slope of the background collected from 2500 to 3700 cm^{-1} on phosphates has changed, becoming less negative with increasing irradiation. Things seem different for carbonates: the signal collected on the Ca-carbonate, nominally anhydrous, has not changed during exposition to UV. In contrast, the exposure to UV has been responsible for the non detection of the Raman peaks related to structural water initially present in the Na and Mg-carbonates, without modifying the slope of the background collected from 2500 to 3700 cm^{-1}.

NIR data are consistent with Raman data. The near-IR spectra of phosphates have not changed that much during the experiments, but only a gentle absorption band related to hydration at 1.9 μm was observed in the spectra of the starting materials. The near-IR spectra of the Ca and Na-carbonates have not changed that much neither during exposure to UV, in contrast to that of the initially hydrated Mg-carbonate (hydromagnesite): the 1.9 μm band related to structural H_2O turned shallower whereas the 1.45 μm, attributed to hydroxyl groups, remained the same, although enlarged, which suggests a possible dehydration of the sample induced by irradiation (or local heating) and/or a creation of electronic defects.

3 Discussion

3.1 Impact of exposure to UV radiation

Although their surface color have become a little more yellow under UV, the Raman spectra of the sulfates, phosphates and carbonates exposed to UV under Mars conditions still exhibit the main feature observed in the Raman spectra of the starting materials, *i.e.*, the peak attributed to the ν_1 symmetric stretching modes. This shows that the minerals investigated here can withstand simulated Martian conditions (including UV radiation) for a certain time, although longer exposure to UV radiation may

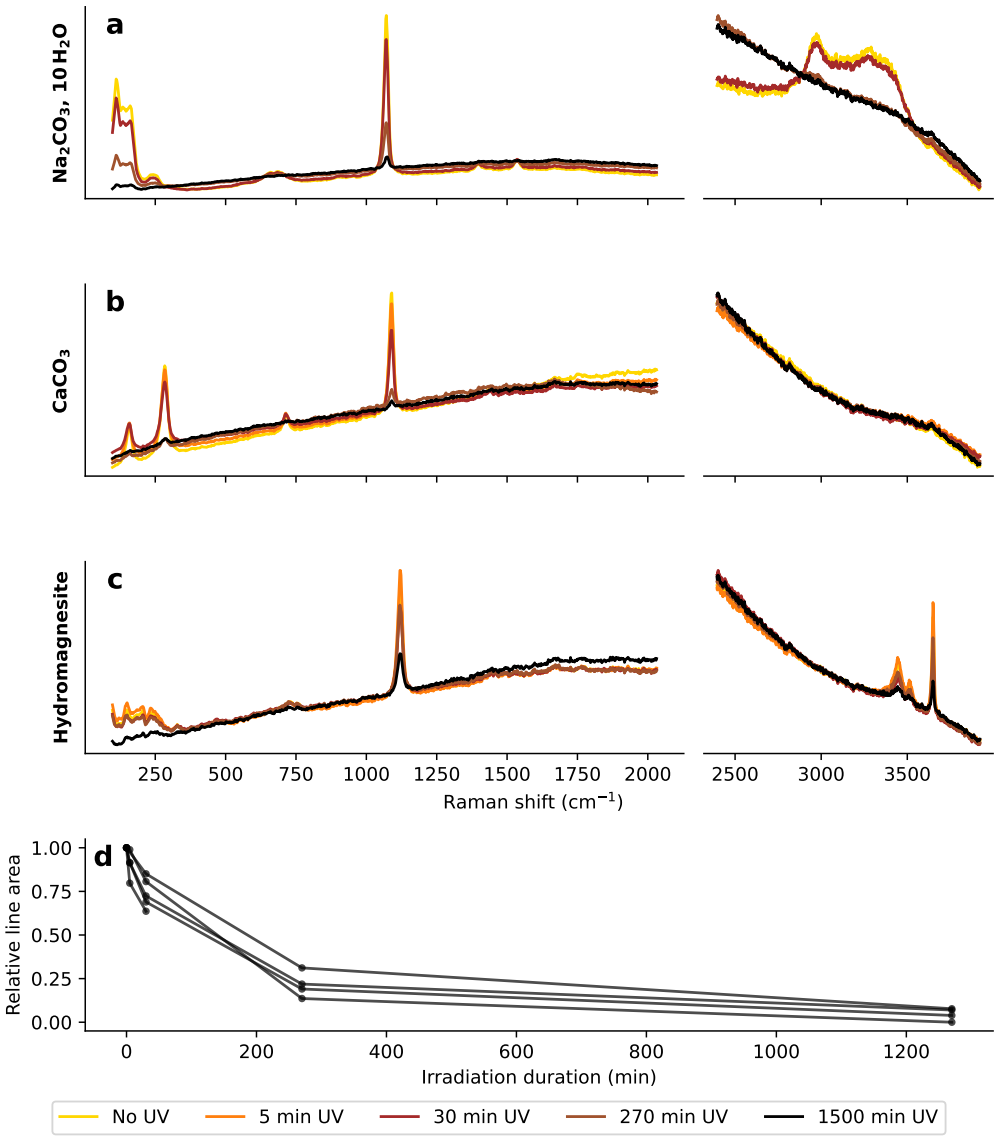

Figure 7: **a** to **c**: Raman spectra of the various carbonate minerals measured with a 2 ns gate. The spectra have been normalized by their total surface to highlight their relative variation. **d**: relative area of each major Raman scattering line as a function of the irradiation duration.

lead to the strong alteration of their structure at the surface, which will strongly affect both IR and Raman signals, as anticipated by earlier experimental studies (Mukhin et al., 1996). The non detection of new peak indicate that no transitory phase nor new species have formed during the experiments. Still, a short exposure to UV has been responsible for a strong increase of the luminescence signal of all the minerals investigated, and for a strong decrease of their Raman signal relative to the background contribution. As is the case for organics exposed to UV radiation under Mars conditions (Megevand et al., 2021), such evolution could be caused by an increasing concentration of electronic defects

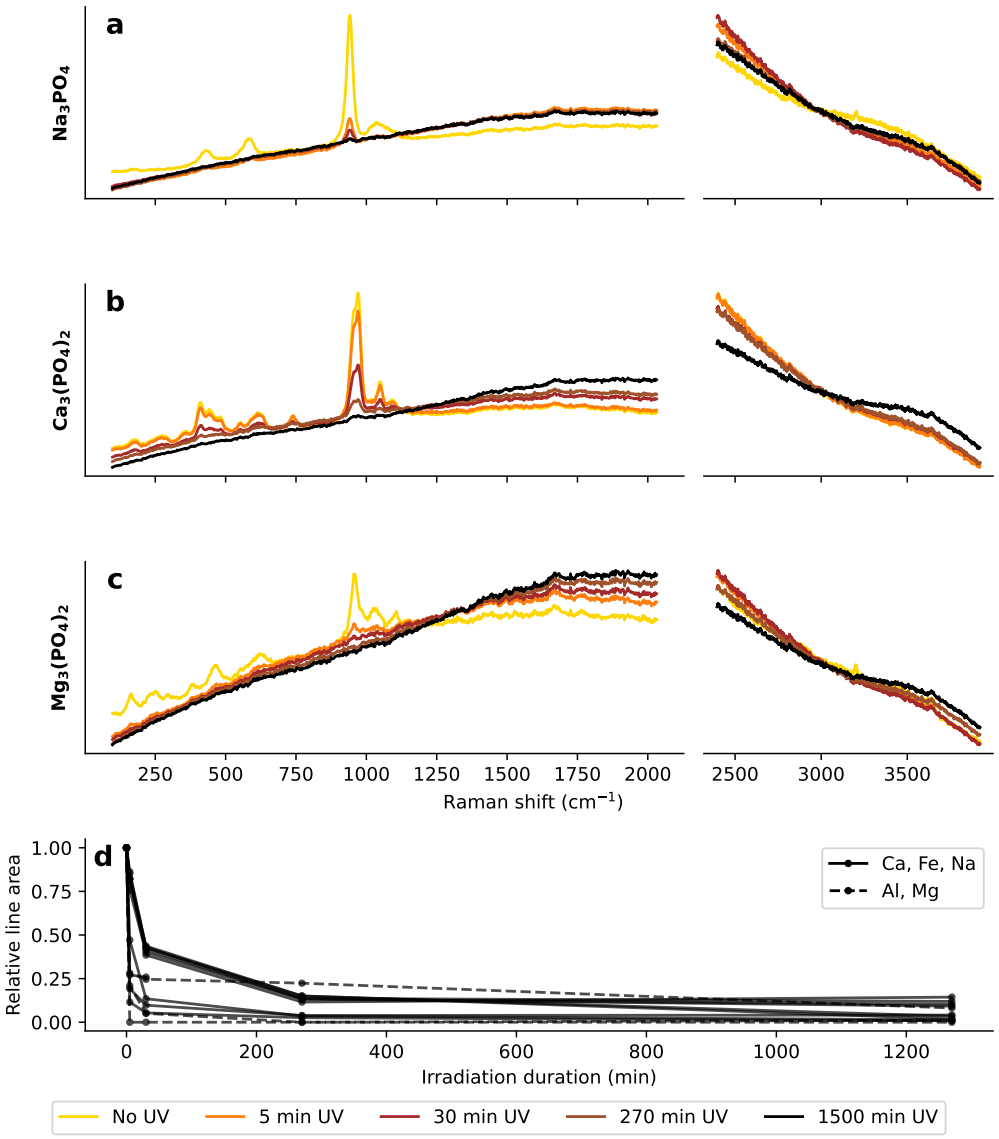

Figure 8: **a** to **c**: Raman spectra of the various phosphate minerals measured with a 2 ns gate. The spectra have been normalized by their total surface to highlight their relative variation. **d**: relative area of each major Raman scattering line as a function of the irradiation duration.

contributing to the background. In fact, previous ESR (Electronic Spin Resonance) investigations have reported the creation of radical species in carbonates exposed to UV light (Bartoll et al., 2000; Kabacińska et al., 2017, 2019). An increase in the concentration of point defects may also explain the broadening of IR bands observed for all samples investigated here, as previously reported for a number of materials exposed to ionizing radiation (*e.g.*, Fourdrin et al. 2009; Megevand et al. 2021. Of note, these defects do not seem to be luminescing centers: concentration quenching would decrease the lifetime of luminescence, as reported for both organic and inorganic materials (Chen and Knutson,

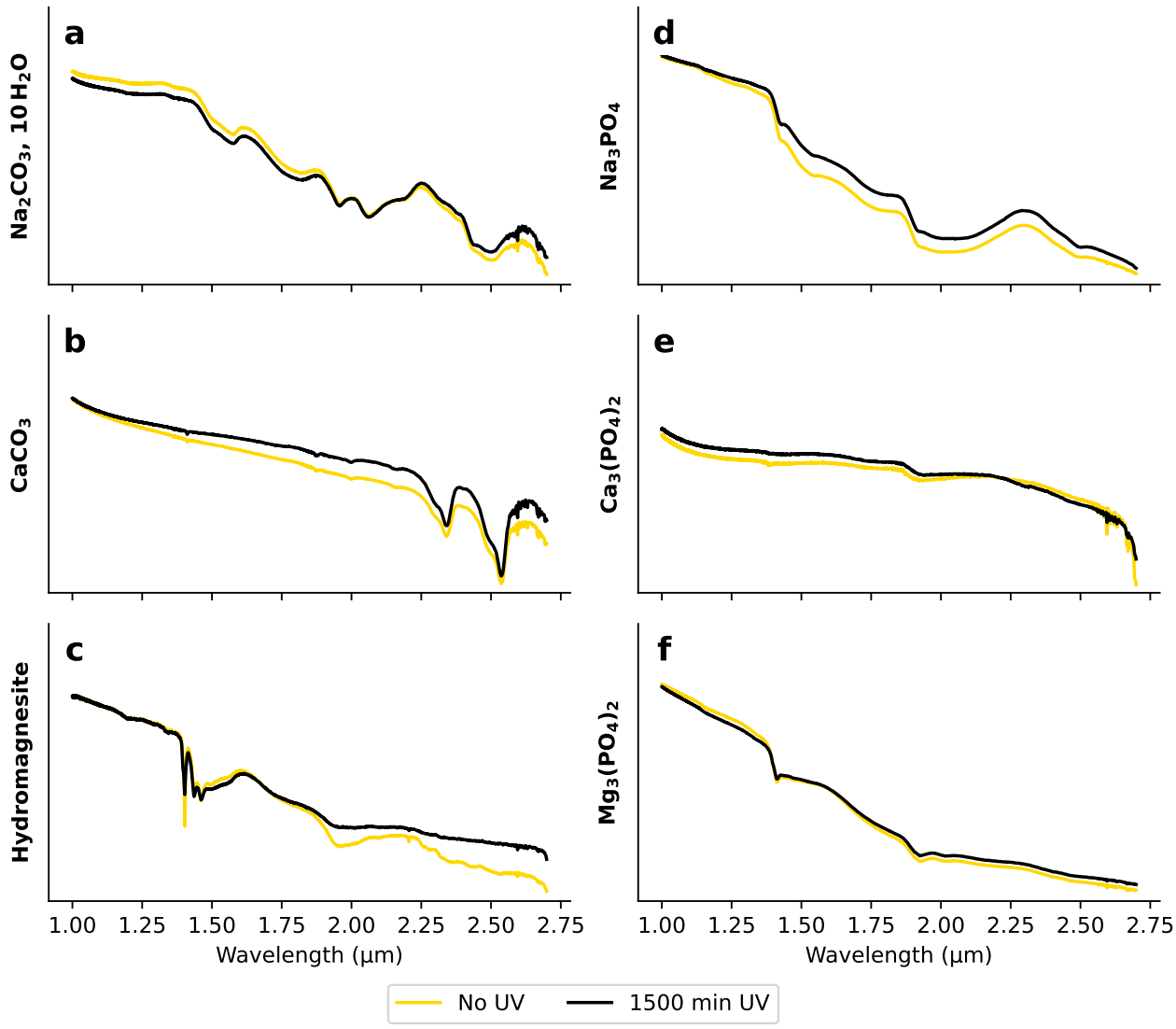

Figure 9: Near-infrared spectra of carbonates (**a** to **c**) and phosphates (**d** to **f**).

1988; Ju et al., 2013; Meza et al., 2014; Green and Buckley, 2014; Fau et al., 2022). But such concentration quenching does not seem to occur here since the lifetime of the luminescence signal does not change with increasing duration of exposure to UV radiation. The decrease of the Raman signal may be due to the radiolysis of chemical bonds or the formation of electronic point defects, the accumulation of radiation damages possibly leading to modifications of the chemical composition and periodicity of the mineral structure. Note that such a decrease may also be related to the strong increase of the background contribution, eventually obscuring the Raman signal.

Of note, all initially hydrated starting materials do not show anymore Raman features attributed to hydration at the end of the present experiments. Yet, neither Morris and Lauer (1980) nor Yen

et al. (1999) observed UV photodehydration, but Bonales et al. (2022) experimentally showed that exposure to UV enhances the kinetics of dehydration. Dehydration may be a direct consequence of the simulated Martian conditions. In fact, Bishop and Pieters (1995) showed that minerals may dehydrate when only exposed to low partial pressure of H_2O. Here, all the samples investigated have been exposed to the pressure and temperature conditions of the experiments for 15 hours before being exposed to UV radiation, and no dehydration was observed during this time. Dehydration may also result from an increase of the sample surface temperature under exposure to the lamp flux, as reported by Morris and Lauer (1980) while relying on an IR-rich Xe(A) radiation responsible for a large increase ($>$ 500°C) of the surface temperature of rather dark samples such as goethite and lepidocrocite. Yet, the rather low flux generated by the lamp used for the present study ($\sim$ 100 times less intense than that of Morris and Lauer (1980)) and the efficient filtering of radiations $>$ 3 µm of the fused silica glass window (leading to a dose delivered to the surface of the samples as low as the dose delivered by the Sun to the surface of Mars) likely prevented thermal dehydration, especially given that the temperature was regulated during the experiments. In fact, although the temperature of the chamber and of the sample holder may increase of 20 to 30°C under exposure to the lamp in the absence of thermal regulation, no such increase was observed during the experiments conducted under thermal regulation. Rather than indicating the dehydration of the samples initially hydrated, the total disappearance of the Raman water bands at about 3400 cm^{-1} of all the samples initially hydrated most likely result from the strong increase of the background which eventually masks the Raman signal over the 3000 to 4000 cm^{-1} spectral window. Still, clear differences exist between the water bands present in the near-IR spectra of the starting materials and those of the samples having been exposed to UV radiation, suggesting that dehydration, structural alteration, or both did occur during the experiments. It remains however difficult to directly relate Raman and IR observations since the volume actually probed by each technique is different. Worse, it is likely that the total volume of sample actually probed and contributing to the Raman or IR signals collected are different for the starting materials and for the samples exposed to UV. In fact, although slight, the change in color of the samples investigated likely reduces their transparency, thus limiting the penetration of the laser and incident light for IR. A partial structural alteration would also reduce the optical penetration depth and therefore the contribution of pristine materials to the total signals.

Another pending question resides in the volume *in fine* affected by UV itself. During exposure

to UV radiation, only the near surface of the samples investigated is penetrated by UV photons (Fornaro et al., 2018; Fox et al., 2019). However, the actual thickness irradiated can vary from one sample to another depending on their optical properties, as the volume of sample actually contributing the Raman and IR signals. Plus, it is very likely that a volume of pristine (non-irradiated) material contributes to each of the measurements reported here, and that this volume decreases with increasing duration of exposure to UV as a result of the reduction of the transparency, either due to a color change or a structural alteration. As a result, it remains difficult to properly quantify the effect of exposure to UV for the samples investigated here. Both the increase of the background, likely related to the increasing creation of defects in the irradiated volume, and the decrease of the Raman signal, likely compensated by the contribution of a volume of pristine material, may be artifactually minimized. The same is true for IR, although the respective volumes of pristine and irradiated materials contributing to the signals may be greater thanks to longer wavelength. Properly quantifying the impact of UV radiation of the spectral signatures of sulfates, phosphates and carbonates would require a dedicated sample preparation ensuring that the entirety of each sample has been interacted with UV photons. At that point, a still pending difficulty would be to have a sufficient volume of sample to properly measure its spectral signature. In any case, it should be kept in mind that although no quantitative data can be provided here, the experimental setup adopted for the present study mimics pretty well Martian conditions in terms of UV radiation and signal collection.

3.2 Implications for the ongoing exploration of Mars

The present results have strong implications for the ongoing exploration of Mars. In fact, most of the surface of Mars is continuously exposed to UV radiation, and it has been the case for quite a long time. Therefore, one should not expect to detect pristine materials, except for measurements on freshly exposed surfaces, for which the timescale of analysis will be highly critical: the faster after excavation, the better. Even 24h of irradiation may be enough to impact the Raman and IR spectral signatures of any target. Therefore, measurements on abraded patches on Mars should be done at latest a Sol after the abrasion to prevent any radiation-induced modifications of the rocks investigated. As shown here, the identification of sulfates, phosphates and carbonates can be compromised if they experienced UV radiation for any given time. Sulfates have been widely detected on the Martian surface, either from orbit in Valles Marineris, Margaritifer Sinus, and Meridiani Planum (Bishop et al., 2004; Vaniman

et al., 2004; Bibring et al., 2005; Gendrin et al., 2005; Lane et al., 2007) or *in situ* by rovers again in Meridiani Planum, Endeavour Crater and Gale Crater (Squyres et al., 2004a,b; Crumpler et al., 2015; Rapin et al., 2016), and also at Jezero crater by *Perseverance* (Clavé et al., 2023). A precise identification of the detected sulfate species has strong implications on their formation conditions (*e.g.* Rapin et al. 2016). For instance, the detection of bassanite rather than that of anhydrite or gypsum, will be interpreted as indicating very specific local conditions in particular regarding water salinity (Rapin et al., 2016). The same is true for phosphates and carbonates (Pollack et al., 1990; Calvin et al., 1994; Clavé et al., 2023). But, as shown here, the modification of their spectral signatures due to UV radiation may bias their identification and/or the estimate of their abundances in rocks, which is directly based on the spectral responses of targets investigated. Similarly, their measured hydration states may not reflect their true/original hydration state. Because both the abundances and the hydration states of sulfates, phosphates and carbonates are critical for Martian paleoenvironmental reconstructions, the effects of exposure to UV have to be taken into account to prevent potentially significant biases.

The present study also highlights that luminescence signals have to be interpreted with special care. A strong and short-lived luminescence signal resembling the ones collected here on irradiated sulfates, phosphates and carbonates may easily be misinterpreted as organic fluorescence. In fact, the very short lifetime of the intrinsic molecular fluorescence of organic compounds (*e.g.*, nanoseconds) compared to most mineral luminescence (micro- to milliseconds), makes it supposedly pertinent to rely on luminescence signals to unambiguously identify organics, as done by Scheller et al. (2022b). However, the short-lived luminescence signals measured here have nothing to do with organics, even though organics may also exhibit such short-lived luminescence signals after exposure to UV (Megevand et al., 2021). On Mars, a solution to ensure interpretations could be to repeat any questionable measurement after a certain time, especially for data collected on freshly excavated surfaces. Obviously, the only proper way to interpret any data is to do it with caution, knowing that most of the answers will be provided by the samples which will be brought back to Earth by the upcoming MSR mission.

4 Conclusion

Altogether, although not quantitative, the present results evidence that exposure to UV has a significant effect on the Raman and IR spectral signatures of sulfates, phosphates and carbonates, which has, in turn, strong implications for the ongoing exploration of Mars. As a precaution, all the targets measured on Mars should be considered as having been exposed to UV radiation to some extent. This will prevent any misinterpretation regarding the nature, abundances and water content of the mineral phases in presence. Of note, the potential impact of additional processes should also be investigated and taken into account for the proper interpretation of existing and future data. In fact, the (sub)surface of Mars is not only exposed to UV radiation, but is also bombarded by gamma-rays, solar energetic protons and galactic cosmic rays which are not absorbed by the thin CO_2 atmosphere and may interact with rocks lying at the surface (Kminek and Bada, 2006; Dartnell et al., 2007; Hassler et al., 2014; Fox et al., 2019). The widespread presence of dust could also generate a strong background blurring Raman signals (Maurice and Wiens, 2021; Wiens et al., 2021). In addition, a number of other ageing processes likely act simultaneously at the surface of Mars, including oxidation (Lasne et al., 2016) and degradation induced by fluid circulation (Viennet et al., 2019), the impact of these processes on sulfates, phosphates and carbonates (as well as on phyllosilicates and organic compounds) remaining to be constrained to properly reconstruct Martian paleoenvironments and optimize the search for traces of life on Mars.

Acknowledgments

We acknowledge the support of the IMPMC spectroscopy platform. We acknowledge financial support from CNRS INP (PI: O. Beyssac), the program Emergences Alliance Sorbonne Universitet (Project MarsAtLab PI: S. Bernard), the program Convergence Sorbonne Université (Project Parimicrobial, PI: K. Benzerara), and from the Institut des Materiaux Sorbonne Universite IMat (Project Ageing on Mars - PI: S. Bernard).

Competing interests

The authors declare that they have no competing interests.

Open research

All the data supporting this study are available upon request.

References

Bartoll, J., Stößer, R., and Nofz, M. (2000). Generation and conversion of electronic defects in calcium carbonates by UV/Vis light. *Applied Radiation and Isotopes*, 52(5):1099–1105.

Ben Mabrouk, K., Kauffmann, T. H., Aroui, H., and Fontana, M. D. (2013). Raman study of cation effect on sulfate vibration modes in solid state and in aqueous solutions. *Journal of Raman Spectroscopy*, 44(11):1603–1608.

Beyssac, O., Forni, O., Cousin, A., Udry, A., Kah, L., Mandon, L., Clavé, E., Liu, Y., Poulet, F., Quantin Nataf, C., Gasnault, O., Johnson, J., Benzerara, K., Beck, P., Dehouck, E., Mangold, N., Alvarez Llamas, C., Anderson, R., Arana, G., Barnes, R., Bernard, S., Bosak, T., Brown, A., Castro, K., Chide, B., Clegg, S., Cloutis, E., Fouchet, T., Gabriel, T., Gupta, S., Lacombe, G., Lasue, J., Le Mouelic, S., Lopez-Reyes, G., Madariaga, J., McCubbin, F., McLennan, S., Manrique, J., Meslin, P., Montmessin, F., Núñez, J., Ollila, A., Ostwald, A., Pilleri, P., Pinet, P., Royer, C., Sharma, S., Schröder, S., Simon, J., Toplis, M., Veneranda, M., Willis, P., Maurice, S., Wiens, R., and Team, T. S. (2023). Petrological traverse of the olivine cumulate Séítah formation at Jezero crater, Mars : A perspective from SuperCam onboard Perseverance. *Journal of Geophysical Research: Planets*, n/a(128):e2022JE007638.

Bhartia, R., Beegle, L. W., DeFlores, L., Abbey, W., Razzell Hollis, J., Uckert, K., Monacelli, B., Edgett, K. S., Kennedy, M. R., Sylvia, M., Aldrich, D., Anderson, M., Asher, S. A., Bailey, Z., Boyd, K., Burton, A. S., Caffrey, M., Calaway, M. J., Calvet, R., Cameron, B., Caplinger, M. A., Carrier, B. L., Chen, N., Chen, A., Clark, M. J., Clegg, S., Conrad, P. G., Cooper, M., Davis, K. N., Ehlmann, B., Facto, L., Fries, M. D., Garrison, D. H., Gasway, D., Ghaemi, F. T., Graff, T. G., Hand, K. P., Harris, C., Hein, J. D., Heinz, N., Herzog, H., Hochberg, E., Houck, A., Hug, W. F., Jensen, E. H., Kah, L. C., Kennedy, J., Krylo, R., Lam, J., Lindeman, M., McGlown, J., Michel, J., Miller, E., Mills, Z., Minitti, M. E., Mok, F., Moore, J., Nealson, K. H., Nelson, A., Newell, R., Nixon, B. E., Nordman, D. A., Nuding, D., Orellana, S., Pauken, M., Peterson, G., Pollock, R.,

412 Quinn, H., Quinto, C., Ravine, M. A., Reid, R. D., Riendeau, J., Ross, A. J., Sackos, J., Schaffner,
413 J. A., Schwochert, M., O Shelton, M., Simon, R., Smith, C. L., Sobron, P., Steadman, K., Steele,
414 A., Thiessen, D., Tran, V. D., Tsai, T., Tuite, M., Tung, E., Wehbe, R., Weinberg, R., Weiner,
415 R. H., Wiens, R. C., Williford, K., Wollonciej, C., Wu, Y.-H., Yingst, R. A., and Zan, J. (2021).
416 Perseverance's Scanning Habitable Environments with Raman and Luminescence for Organics and
417 Chemicals (SHERLOC) Investigation. *Space Science Reviews*, 217(4):58.

418 Bibring, J.-P., Hamm, V., Pilorget, C., Vago, J. L., and the MicrOmega Team (2017). The MicrOmega
419 Investigation Onboard ExoMars. *Astrobiology*, 17(6-7):621–626.

420 Bibring, J.-P., Langevin, Y., Gendrin, A., Gondet, B., Poulet, F., Berthe, M., Soufflot, A., Arvidson,
421 R., Mangold, N., Mustard, J., Drossart, P., Team, O., Erard, S., Forni, O., Combes, M., Encrenaz,
422 T., Fouchet, T., Merchiorri, R., Belluci, G., Altieri, F., Formisano, V., Bonello, G., Capaccioni, F.,
423 Cerroni, P., Coradini, A., Fonti, S., Kottsov, V., Ignatiev, N., Moroz, V., Titov, D., Zasova, L.,
424 Mangold, M., Pinet, P., Doute, S., Schmitt, B., Sotin, C., Hauber, E., Hoffmann, H., Jaumann,
425 R., Keller, U., Duxbury, T., and Forget, F. (2005). Mars Surface Diversity as Revealed by the
426 OMEGA/Mars Express Observations. *Science*, 307(5715):1576.

427 Bish, D. L., William Carey, J., Vaniman, D. T., and Chipera, S. J. (2003). Stability of hydrous
428 minerals on the martian surface. *Icarus*, 164:96–103.

429 Bishop, J. L., Darby Dyar, M., Lane, M. D., and Banfield, J. F. (2004). Spectral identification of
430 hydrated sulfates on Mars and comparison with acidic environments on Earth. *International Journal*
431 *of Astrobiology*, 3:275–285.

432 Bishop, J. L. and Pieters, C. M. (1995). Low-temperature and low atmospheric pressure infrared
433 reflectance spectroscopy of Mars soil analog materials. *Journal of Geophysical Research*, 100:5369–
434 5380.

435 Bonales, L. J., Rodríguez-Villagra, N., Fernandez-Sampedro, M., and Mateo-Martí, E. (2022). De-
436 hydration rate of the glycine-MgSO 4 ·5H 2 O complex and the stability of glycine expelled from
437 the complex by in situ Raman spectroscopy under Mars-relevant conditions. *Journal of Raman*
438 *Spectroscopy*, 53:724–734.

Buzgar, N., Buzatu, A., and Sanislav, I. V. (2009). The Raman Study of Certain Sulfates. *Analele Stiintifice Ale Universitatii „AL. I. CUZA" Iasi*, 55(1):19.

Calvin, W. M., King, T. V. V., and Clark, R. N. (1994). Hydrous carbonates on Mars?: Evidence from Mariner 6/7 infrared spectrometer and ground-based telescopic spectra. *Journal of Geophysical Research*, 99:14659–14676.

Carrier, B. L., Abbey, W. J., Beegle, L. W., Bhartia, R., and Liu, Y. (2019). Attenuation of Ultraviolet Radiation in Rocks and Minerals: Implications for Mars Science. *Journal of Geophysical Research: Planets*, 124(10):2599–2612.

Carter, J., Poulet, F., Bibring, J.-P., and Murchie, S. (2010). Detection of Hydrated Silicates in Crustal Outcrops in the Northern Plains of Mars. *Science*, 328(5986):1682–1686.

Chen, R. F. and Knutson, J. R. (1988). Mechanism of fluorescence concentration quenching of carboxyfluorescein in liposomes: Energy transfer to nonfluorescent dimers. *Analytical Biochemistry*, 172(1):61–77.

Clavé, E., Benzerara, K., Meslin, P.-Y., Forni, O., Royer, C., Mandon, L., Beck, P., Quantin-Nataf, C., Beyssac, O., Cousin, A., Bousquet, B., Wiens, R., Maurice, S., Dehouck, E., Schröder, S., Gasnault, O., Mangold, N., Dromart, G., Bosak, T., Bernard, S., Udry, A., Anderson, R., Arana, G., Brown, A., Castro, K., Clegg, S., Cloutis, E., Fairén, A., Flannery, D., Gasda, P., Johnson, J., Lasue, J., Lopez-Reyes, G., Madariaga, J., Manrique, J., Le Mouélic, S., Núñez, J., Ollila, A., Pilleri, P., Pilorget, C., Pinet, P., Poulet, F., Veneranda, M., Wolf, Z., and Team, t. S. (2023). Carbonate Detection with SuperCam in Igneous Rocks on the floor of Jezero Crater, Mars. *Journal of Geophysical Research: Planets*, 128(1).

Cloutis, E. A., Craig, M. A., Kruzelecky, R. V., Jamroz, W. R., Scott, A., Hawthorne, F. C., and Mertzman, S. A. (2008). Spectral reflectance properties of minerals exposed to simulated Mars surface conditions. *Icarus*, 195(1):140–168.

Cloutis, E. A., Craig, M. A., Mustard, J. F., Kruzelecky, R. V., Jamroz, W. R., Scott, A., Bish, D. L., Poulet, F., Bibring, J.-P., and King, P. L. (2007). Stability of hydrated minerals on Mars. *Geophysical Research Letters*, 34(20).

Crumpler, L. S., Arvidson, R. E., Bell, J., Clark, B. C., Cohen, B. A., Farrand, W. H., Gellert, R., Golombek, M., Grant, J. A., Guinness, E., Herkenhoff, K. E., Johnson, J. R., Jolliff, B., Ming, D. W., Mittlefehldt, D. W., Parker, T., Rice, J. W., Squyres, S. W., Sullivan, R., and Yen, A. S. (2015). Context of ancient aqueous environments on Mars from in situ geologic mapping at Endeavour Crater. *Journal of Geophysical Research: Planets*, 120(3):538–569.

Dartnell, L. R., Desorgher, L., Ward, J. M., and Coates, A. J. (2007). Modelling the surface and subsurface Martian radiation environment: Implications for astrobiology. *Geophysical Research Letters*, 34(2).

Ehlmann, B. L., Mustard, J. F., Murchie, S. L., Bibring, J.-P., Meunier, A., Fraeman, A. A., and Langevin, Y. (2011). Subsurface water and clay mineral formation during the early history of Mars. *Nature*, 479(7371):53–60.

Farley, K. A., Williford, K. H., Stack, K. M., Bhartia, R., Chen, A., de la Torre, M., Hand, K., Goreva, Y., Herd, C. D. K., Hueso, R., Liu, Y., Maki, J. N., Martinez, G., Moeller, R. C., Nelessen, A., Newman, C. E., Nunes, D., Ponce, A., Spanovich, N., Willis, P. A., Beegle, L. W., Bell, J. F., Brown, A. J., Hamran, S.-E., Hurowitz, J. A., Maurice, S., Paige, D. A., Rodriguez-Manfredi, J. A., Schulte, M., and Wiens, R. C. (2020). Mars 2020 Mission Overview. *Space Science Reviews*, 216(8):142.

Fau, A., Beyssac, O., Gauthier, M., Meslin, P. Y., Cousin, A., Benzerara, K., Bernard, S., Boulliard, J. C., Gasnault, O., Forni, O., Wiens, R. C., Morand, M., Rosier, P., Garino, Y., Pont, S., and Maurice, S. (2019). Pulsed laser-induced heating of mineral phases: Implications for laser-induced breakdown spectroscopy combined with Raman spectroscopy. *Spectrochimica Acta Part B: Atomic Spectroscopy*, 160:105687.

Fau, A., Beyssac, O., Gauthier, M., Panczer, G., Gasnault, O., Meslin, P.-Y., Bernard, S., Maurice, S., Forni, O., Boulliard, J.-C., Bosc, F., and Drouet, C. (2022). Time-resolved Raman and luminescence spectroscopy of synthetic REE-doped hydroxylapatites and natural apatites. *American Mineralogist*, 107:1341–1352.

Fornaro, T., Boosman, A., Brucato, J. R., ten Kate, I. L., Siljeström, S., Poggiali, G., Steele, A., and Hazen, R. M. (2018). UV irradiation of biomarkers adsorbed on minerals under Martian-like conditions: Hints for life detection on Mars. *Icarus*, 313:38–60.

494 Fouchet, T., Reess, J.-M., Montmessin, F., Hassen-Khodja, R., Nguyen-Tuong, N., Humeau, O.,
495 Jacquinod, S., Lapauw, L., Parisot, J., Bonafous, M., Bernardi, P., Chapron, F., Jeanneau, A.,
496 Collin, C., Zeganadin, D., Nibert, P., Abbaki, S., Montaron, C., Blanchard, C., Arslanyan, V.,
497 Achelhi, O., Colon, C., Royer, C., Hamm, V., Beuzit, M., Poulet, F., Pilorget, C., Mandon, L., Forni,
498 O., Cousin, A., Gasnault, O., Pilleri, P., Dubois, B., Quantin, C., Beck, P., Beyssac, O., Le Mouélic,
499 S., Johnsson, J. R., McConnochie, T. H., Maurice, S., and Wiens, R. C. (2022). The SuperCam
500 infrared spectrometer for the perseverance rover of the Mars2020 mission. *Icarus*, 373:114773.

501 Fourdrin, C., Balan, E., Allard, T., Boukari, C., and Calas, G. (2009). Induced modifications of
502 kaolinite under ionizing radiation: An infrared spectroscopic study. *Physics and Chemistry of*
503 *Minerals*, 36:291–299.

504 Fox, A. C., Eigenbrode, J. L., and Freeman, K. H. (2019). Radiolysis of Macromolecular Organic Ma-
505 terial in Mars-Relevant Mineral Matrices. *Journal of Geophysical Research: Planets*, 124(12):3257–
506 3266.

507 Gendrin, A., Mangold, N., Bibring, J.-P., Langevin, Y., Gondet, B., Poulet, F., Bonello, G., Quantin,
508 C., Mustard, J., Arvidson, R., and LeMouélic, S. (2005). Sulfates in Martian Layered Terrains: The
509 OMEGA/Mars Express View. *Science*, 307(5715):1587–1591.

510 Green, A. P. and Buckley, A. R. (2014). Solid state concentration quenching of organic fluorophores in
511 PMMA. *Physical Chemistry Chemical Physics (Incorporating Faraday Transactions)*, 17:1435–1440.

512 Grotzinger, J. P., Sumner, D. Y., Kah, L. C., Stack, K., Gupta, S., Edgar, L., Rubin, D., Lewis, K.,
513 Schieber, J., Mangold, N., Milliken, R., Conrad, P. G., DesMarais, D., Farmer, J., Siebach, K.,
514 Calef, F., Hurowitz, J., McLennan, S. M., Ming, D., Vaniman, D., Crisp, J., Vasavada, A., Edgett,
515 K. S., Malin, M., Blake, D., Gellert, R., Mahaffy, P., Wiens, R. C., Maurice, S., Grant, J. A.,
516 Wilson, S., Anderson, R. C., Beegle, L., Arvidson, R., Hallet, B., Sletten, R. S., Rice, M., Bell, J.,
517 Griffes, J., Ehlmann, B., Anderson, R. B., Bristow, T. F., Dietrich, W. E., Dromart, G., Eigenbrode,
518 J., Fraeman, A., Hardgrove, C., Herkenhoff, K., Jandura, L., Kocurek, G., Lee, S., Leshin, L. A.,
519 Leveille, R., Limonadi, D., Maki, J., McCloskey, S., Meyer, M., Minitti, M., Newsom, H., Oehler,
520 D., Okon, A., Palucis, M., Parker, T., Rowland, S., Schmidt, M., Squyres, S., Steele, A., Stolper,
521 E., Summons, R., Treiman, A., Williams, R., Yingst, A., Team, M. S., Kemppinen, O., Bridges,

N., Johnson, J. R., Cremers, D., Godber, A., Wadhwa, M., Wellington, D., McEwan, I., Newman, C., Richardson, M., Charpentier, A., Peret, L., King, P., Blank, J., Weigle, G., Li, S., Robertson, K., Sun, V., Baker, M., Edwards, C., Farley, K., Miller, H., Newcombe, M., Pilorget, C., Brunet, C., Hipkin, V., Léveillé, R., Marchand, G., Sánchez, P. S., Favot, L., Cody, G., Flückiger, L., Lees, D., Nefian, A., Martin, M., Gailhanou, M., Westall, F., Israël, G., Agard, C., Baroukh, J., Donny, C., Gaboriaud, A., Guillemot, P., Lafaille, V., Lorigny, E., Paillet, A., Pérez, R., Saccoccio, M., Yana, C., Armiens-Aparicio, C., Rodríguez, J. C., Blázquez, I. C., Gómez, F. G., Gómez-Elvira, J., Hettrich, S., Malvitte, A. L., Jiménez, M. M., Martínez-Frías, J., Martín-Soler, J., Martín-Torres, F. J., Jurado, A. M., Mora-Sotomayor, L., Caro, G. M., López, S. N., Peinado-González, V., Pla-García, J., Manfredi, J. A. R., Romeral-Planelló, J. J., Fuentes, S. A. S., Martinez, E. S., Redondo, J. T., Urqui-O'Callaghan, R., Mier, M.-P. Z., Chipera, S., Lacour, J.-L., Mauchien, P., Sirven, J.-B., Manning, H., Fairén, A., Hayes, A., Joseph, J., Sullivan, R., Thomas, P., Dupont, A., Lundberg, A., Melikechi, N., Mezzacappa, A., DeMarines, J., Grinspoon, D., Reitz, G., Prats, B., Atlaskin, E., Genzer, M., Harri, A.-M., Haukka, H., Kahanpää, H., Kauhanen, J., Paton, M., Polkko, J., Schmidt, W., Siili, T., Fabre, C., Wray, J., Wilhelm, M. B., Poitrasson, F., Patel, K., Gorevan, S., Indyk, S., Paulsen, G., Bish, D., Gondet, B., Langevin, Y., Geffroy, C., Baratoux, D., Berger, G., Cros, A., d'Uston, C., Forni, O., Gasnault, O., Lasue, J., Lee, Q.-M., Meslin, P.-Y., Pallier, E., Parot, Y., Pinet, P., Schröder, S., Toplis, M., Lewin, É., Brunner, W., Heydari, E., Achilles, C., Sutter, B., Cabane, M., Coscia, D., Szopa, C., Robert, F., Sautter, V., Le Mouélic, S., Nachon, M., Buch, A., Stalport, F., Coll, P., François, P., Raulin, F., Teinturier, S., Cameron, J., Clegg, S., Cousin, A., DeLapp, D., Dingler, R., Jackson, R. S., Johnstone, S., Lanza, N., Little, C., Nelson, T., Williams, R. B., Jones, A., Kirkland, L., Baker, B., Cantor, B., Caplinger, M., Davis, S., Duston, B., Fay, D., Harker, D., Herrera, P., Jensen, E., Kennedy, M. R., Krezoski, G., Krysak, D., Lipkaman, L., McCartney, E., McNair, S., Nixon, B., Posiolova, L., Ravine, M., Salamon, A., Saper, L., Stoiber, K., Supulver, K., Van Beek, J., Van Beek, T., Zimdar, R., French, K. L., Iagnemma, K., Miller, K., Goesmann, F., Goetz, W., Hviid, S., Johnson, M., Lefavor, M., Lyness, E., Breves, E., Dyar, M. D., Fassett, C., Edwards, L., Haberle, R., Hoehler, T., Hollingsworth, J., Kahre, M., Keely, L., McKay, C., Bleacher, L., Brinckerhoff, W., Choi, D., Dworkin, J. P., Floyd, M., Freissinet, C., Garvin, J., Glavin, D., Harpold, D., Martin, D. K., McAdam, A., Pavlov, A., Raaen, E., Smith, M. D., Stern, J., Tan, F., Trainer, M., Posner, A., Voytek, M., Aubrey, A., Behar, A., Blaney, D.,

552 Brinza, D., Christensen, L., DeFlores, L., Feldman, J., Feldman, S., Flesch, G., Jun, I., Keymeulen,
553 D., Mischna, M., Morookian, J. M., Pavri, B., Schoppers, M., Sengstacken, A., Simmonds, J. J.,
554 Spanovich, N., Juarez, M. d. l. T., Webster, C. R., Yen, A., Archer, P. D., Cucinotta, F., Jones, J. H.,
555 Morris, R. V., Niles, P., Rampe, E., Nolan, T., Fisk, M., Radziemski, L., Barraclough, B., Bender,
556 S., Berman, D., Dobrea, E. N., Tokar, R., Cleghorn, T., Huntress, W., Manhès, G., Hudgins, J.,
557 Olson, T., Stewart, N., Sarrazin, P., Vicenzi, E., Bullock, M., Ehresmann, B., Hamilton, V., Hassler,
558 D., Peterson, J., Rafkin, S., Zeitlin, C., Fedosov, F., Golovin, D., Karpushkina, N., Kozyrev, A.,
559 Litvak, M., Malakhov, A., Mitrofanov, I., Mokrousov, M., Nikiforov, S., Prokhorov, V., Sanin,
560 A., Tretyakov, V., Varenikov, A., Vostrukhin, A., Kuzmin, R., Clark, B., Wolff, M., Botta, O.,
561 Drake, D., Bean, K., Lemmon, M., Schwenzer, S. P., Lee, E. M., Sucharski, R., Hernández, M. Á.
562 d. P., Ávalos, J. J. B., Ramos, M., Kim, M.-H., Malespin, C., Plante, I., Muller, J.-P., Navarro-
563 González, R., Ewing, R., Boynton, W., Downs, R., Fitzgibbon, M., Harshman, K., Morrison, S.,
564 Kortmann, O., Williams, A., Lugmair, G., Wilson, M. A., Jakosky, B., Balic-Zunic, T., Frydenvang,
565 J., Jensen, J. K., Kinch, K., Koefoed, A., Madsen, M. B., Stipp, S. L. S., Boyd, N., Campbell, J. L.,
566 Perrett, G., Pradler, I., VanBommel, S., Jacob, S., Owen, T., Savijärvi, H., Boehm, E., Böttcher, S.,
567 Burmeister, S., Guo, J., Köhler, J., García, C. M., Mueller-Mellin, R., Wimmer-Schweingruber, R.,
568 Bridges, J. C., McConnochie, T., Benna, M., Franz, H., Bower, H., Brunner, A., Blau, H., Boucher,
569 T., Carmosino, M., Atreya, S., Elliott, H., Halleaux, D., Rennó, N., Wong, M., Pepin, R., Elliott,
570 B., Spray, J., Thompson, L., Gordon, S., Ollila, A., Williams, J., Vasconcelos, P., Bentz, J., Nealson,
571 K., Popa, R., Moersch, J., Tate, C., Day, M., Francis, R., McCullough, E., Cloutis, E., ten Kate,
572 I. L., Scholes, D., Slavney, S., Stein, T., Ward, J., Berger, J., and Moores, J. E. (2014). A Habitable
573 Fluvio-Lacustrine Environment at Yellowknife Bay, Gale Crater, Mars. *Science*, 343(6169):1242777.

574 Gunasekaran, S., Anbalagan, G., and Pandi, S. (2006). Raman and infrared spectra of carbonates of
575 calcite structure. *Journal of Raman Spectroscopy*, 37(9):892–899.

576 Harner, P. L. and Gilmore, M. S. (2015). Visible–near infrared spectra of hydrous carbonates, with
577 implications for the detection of carbonates in hyperspectral data of Mars. *Icarus*, 250:204–214.

578 Hassler, D. M., Zeitlin, C., Wimmer-Schweingruber, R. F., Ehresmann, B., Rafkin, S., Eigenbrode,
579 J. L., Brinza, D. E., Weigle, G., Böttcher, S., Böhm, E., Burmeister, S., Guo, J., Köhler, J.,
580 Martin, C., Reitz, G., Cucinotta, F. A., Kim, M.-H., Grinspoon, D., Bullock, M. A., Posner, A.,

Gómez-Elvira, J., Vasavada, A., Grotzinger, J. P., Team, M. S., Kemppinen, O., Cremers, D., Bell, J. F., Edgar, L., Farmer, J., Godber, A., Wadhwa, M., Wellington, D., McEwan, I., Newman, C., Richardson, M., Charpentier, A., Peret, L., King, P., Blank, J., Schmidt, M., Li, S., Milliken, R., Robertson, K., Sun, V., Baker, M., Edwards, C., Ehlmann, B., Farley, K., Griffes, J., Miller, H., Newcombe, M., Pilorget, C., Rice, M., Siebach, K., Stack, K., Stolper, E., Brunet, C., Hipkin, V., Léveillé, R., Marchand, G., Sánchez, P. S., Favot, L., Cody, G., Steele, A., Flückiger, L., Lees, D., Nefian, A., Martin, M., Gailhanou, M., Westall, F., Israël, G., Agard, C., Baroukh, J., Donny, C., Gaboriaud, A., Guillemot, P., Lafaille, V., Lorigny, E., Paillet, A., Pérez, R., Saccoccio, M., Yana, C., Armiens-Aparicio, C., Rodríguez, J. C., Blázquez, I. C., Gómez, F. G., Hettrich, S., Malvitte, A. L., Jiménez, M. M., Martínez-Frías, J., Martín-Soler, J., Martín-Torres, F. J., Jurado, A. M., Mora-Sotomayor, L., Caro, G. M., López, S. N., Peinado-González, V., Pla-García, J., Manfredi, J. A. R., Romeral-Planelló, J. J., Fuentes, S. A. S., Martinez, E. S., Redondo, J. T., Urqui-O'Callaghan, R., Mier, M.-P. Z., Chipera, S., Lacour, J.-L., Mauchien, P., Sirven, J.-B., Manning, H., Fairén, A., Hayes, A., Joseph, J., Squyres, S., Sullivan, R., Thomas, P., Dupont, A., Lundberg, A., Melikechi, N., Mezzacappa, A., Berger, T., Matthia, D., Prats, B., Atlaskin, E., Genzer, M., Harri, A.-M., Haukka, H., Kahanpää, H., Kauhanen, J., Kemppinen, O., Paton, M., Polkko, J., Schmidt, W., Siili, T., Fabre, C., Wray, J., Wilhelm, M. B., Poitrasson, F., Patel, K., Gorevan, S., Indyk, S., Paulsen, G., Gupta, S., Bish, D., Schieber, J., Gondet, B., Langevin, Y., Geffroy, C., Baratoux, D., Berger, G., Cros, A., d'Uston, C., Forni, O., Gasnault, O., Lasue, J., Lee, Q.-M., Maurice, S., Meslin, P.-Y., Pallier, E., Parot, Y., Pinet, P., Schröder, S., Toplis, M., Lewin, É., Brunner, W., Heydari, E., Achilles, C., Oehler, D., Sutter, B., Cabane, M., Coscia, D., Israël, G., Szopa, C., Dromart, G., Robert, F., Sautter, V., Le Mouélic, S., Mangold, N., Nachon, M., Buch, A., Stalport, F., Coll, P., François, P., Raulin, F., Teinturier, S., Cameron, J., Clegg, S., Cousin, A., DeLapp, D., Dingler, R., Jackson, R. S., Johnstone, S., Lanza, N., Little, C., Nelson, T., Wiens, R. C., Williams, R. B., Jones, A., Kirkland, L., Treiman, A., Baker, B., Cantor, B., Caplinger, M., Davis, S., Duston, B., Edgett, K., Fay, D., Hardgrove, C., Harker, D., Herrera, P., Jensen, E., Kennedy, M. R., Krezoski, G., Krysak, D., Lipkaman, L., Malin, M., McCartney, E., McNair, S., Nixon, B., Posiolova, L., Ravine, M., Salamon, A., Saper, L., Stoiber, K., Supulver, K., Van Beek, J., Van Beek, T., Zimdar, R., French, K. L., Iagnemma, K., Miller, K., Summons, R., Goesmann, F., Goetz, W., Hviid, S., Johnson, M., Lefavor, M., Lyness, E., Breves, E., Dyar, M. D., Fassett,

C., Blake, D. F., Bristow, T., DesMarais, D., Edwards, L., Haberle, R., Hoehler, T., Hollingsworth, J., Kahre, M., Keely, L., McKay, C., Wilhelm, M. B., Bleacher, L., Brinckerhoff, W., Choi, D., Conrad, P., Dworkin, J. P., Floyd, M., Freissinet, C., Garvin, J., Glavin, D., Harpold, D., Jones, A., Mahaffy, P., Martin, D. K., McAdam, A., Pavlov, A., Raaen, E., Smith, M. D., Stern, J., Tan, F., Trainer, M., Meyer, M., Voytek, M., Anderson, R. C., Aubrey, A., Beegle, L. W., Behar, A., Blaney, D., Calef, F., Christensen, L., Crisp, J. A., DeFlores, L., Ehlmann, B., Feldman, J., Feldman, S., Flesch, G., Hurowitz, J., Jun, I., Keymeulen, D., Maki, J., Mischna, M., Morookian, J. M., Parker, T., Pavri, B., Schoppers, M., Sengstacken, A., Simmonds, J. J., Spanovich, N., Juarez, M. d. l. T., Webster, C. R., Yen, A., Archer, P. D., Jones, J. H., Ming, D., Morris, R. V., Niles, P., Rampe, E., Nolan, T., Fisk, M., Radziemski, L., Barraclough, B., Bender, S., Berman, D., Dobrea, E. N., Tokar, R., Vaniman, D., Williams, R. M. E., Yingst, A., Lewis, K., Leshin, L., Cleghorn, T., Huntress, W., Manhès, G., Hudgins, J., Olson, T., Stewart, N., Sarrazin, P., Grant, J., Vicenzi, E., Wilson, S. A., Hamilton, V., Peterson, J., Fedosov, F., Golovin, D., Karpushkina, N., Kozyrev, A., Litvak, M., Malakhov, A., Mitrofanov, I., Mokrousov, M., Nikiforov, S., Prokhorov, V., Sanin, A., Tretyakov, V., Varenikov, A., Vostrukhin, A., Kuzmin, R., Clark, B., Wolff, M., McLennan, S., Botta, O., Drake, D., Bean, K., Lemmon, M., Schwenzer, S. P., Anderson, R. B., Herkenhoff, K., Lee, E. M., Sucharski, R., Hernández, M. Á. d. P., Ávalos, J. J. B., Ramos, M., Malespin, C., Plante, I., Muller, J.-P., Navarro-González, R., Ewing, R., Boynton, W., Downs, R., Fitzgibbon, M., Harshman, K., Morrison, S., Dietrich, W., Kortmann, O., Palucis, M., Sumner, D. Y., Williams, A., Lugmair, G., Wilson, M. A., Rubin, D., Jakosky, B., Balic-Zunic, T., Frydenvang, J., Jensen, J. K., Kinch, K., Koefoed, A., Madsen, M. B., Stipp, S. L. S., Boyd, N., Campbell, J. L., Gellert, R., Perrett, G., Pradler, I., VanBommel, S., Jacob, S., Owen, T., Rowland, S., Atlaskin, E., Savijärvi, H., García, C. M., Mueller-Mellin, R., Bridges, J. C., McConnochie, T., Benna, M., Franz, H., Bower, H., Brunner, A., Blau, H., Boucher, T., Carmosino, M., Atreya, S., Elliott, H., Halleaux, D., Rennó, N., Wong, M., Pepin, R., Elliott, B., Spray, J., Thompson, L., Gordon, S., Newsom, H., Ollila, A., Williams, J., Vasconcelos, P., Bentz, J., Nealson, K., Popa, R., Kah, L. C., Moersch, J., Tate, C., Day, M., Kocurek, G., Hallet, B., Sletten, R., Francis, R., McCullough, E., Cloutis, E., ten Kate, I. L., Kuzmin, R., Arvidson, R., Fraeman, A., Scholes, D., Slavney, S., Stein, T., Ward, J., Berger, J., and Moores, J. E. (2014). Mars' Surface Radiation Environment Measured with the Mars Science Laboratory's Curiosity Rover. *Science*, 343(6169):1244797.

641 Ju, G., Hu, Y., Chen, L., Wang, X., and Mu, Z. (2013). Concentration quenching of persistent
642 luminescence. *Physica B: Condensed Matter*, 415:1–4.

643 Kabacińska, Z., Krzyminiewski, R., Tadyszak, K., and Coy, E. (2019). Generation of UV-induced
644 radiation defects in calcite. *Quaternary Geochronology*, 51:24–42.

645 Kabacińska, Z., Yate, L., Wencka, M., Krzyminiewski, R., Tadyszak, K., and Coy, E. (2017). Nanoscale
646 Effects of Radiation (UV, X-ray, and γ) on Calcite Surfaces: Implications for its Mechanical and
647 Physico-Chemical Properties. *The Journal of Physical Chemistry C*, 121(24):13357–13369.

648 Kminek, G. and Bada, J. L. (2006). The effect of ionizing radiation on the preservation of amino acids
649 on Mars. *Earth and Planetary Science Letters*, 245(1):1–5.

650 Korablev, O., Montmessin, F., Trokhimovskiy, A., Fedorova, A. A., Shakun, A. V., Grigoriev, A. V.,
651 Moshkin, B. E., Ignatiev, N. I., Forget, F., Lefèvre, F., Anufreychik, K., Dzuban, I., Ivanov, Y. S.,
652 Kalinnikov, Y. K., Kozlova, T. O., Kungurov, A., Makarov, V., Martynovich, F., Maslov, I., Mer-
653 zlyakov, D., Moiseev, P. P., Nikolskiy, Y., Patrakeev, A., Patsaev, D., Santos-Skripko, A., Sazonov,
654 O., Semena, N., Semenov, A., Shashkin, V., Sidorov, A., Stepanov, A. V., Stupin, I., Timonin, D.,
655 Titov, A. Y., Viktorov, A., Zharkov, A., Altieri, F., Arnold, G., Belyaev, D. A., Bertaux, J. L., Bet-
656 sis, D. S., Duxbury, N., Encrenaz, T., Fouchet, T., Gérard, J.-C., Grassi, D., Guerlet, S., Hartogh,
657 P., Kasaba, Y., Khatuntsev, I., Krasnopolsky, V. A., Kuzmin, R. O., Lellouch, E., Lopez-Valverde,
658 M. A., Luginin, M., Määttänen, A., Marcq, E., Martin Torres, J., Medvedev, A. S., Millour, E.,
659 Olsen, K. S., Patel, M. R., Quantin-Nataf, C., Rodin, A. V., Shematovich, V. I., Thomas, I.,
660 Thomas, N., Vazquez, L., Vincendon, M., Wilquet, V., Wilson, C. F., Zasova, L. V., Zelenyi, L. M.,
661 and Zorzano, M. P. (2017). The Atmospheric Chemistry Suite (ACS) of Three Spectrometers for
662 the ExoMars 2016 Trace Gas Orbiter. *Space Science Reviews*, 214(1):7.

663 Lane, M. D., Bishop, J. L., Dyar, M. D., Parente, M., King, P. L., and Hyde, B. C. (2007). Identifying
664 the Phosphate and Ferric Sulfate Minerals in the Paso Robles Soils (Gusev Crater, Mars) Using an
665 Integrated Spectral Approach. *38th Lunar and Planetary Science Conference*, page 2176.

666 Lasne, J., Noblet, A., Szopa, C., Navarro-González, R., Cabane, M., Poch, O., Stalport, F., François,
667 P., Atreya, S., and Coll, P. (2016). Oxidants at the Surface of Mars: A Review in Light of Recent
668 Exploration Results. *Astrobiology*, 16(12):977–996.

669 Manrique, J. A., Lopez-Reyes, G., Cousin, A., Rull, F., Maurice, S., Wiens, R. C., Madsen, M. B.,
670 Madariaga, J. M., Gasnault, O., Aramendia, J., Arana, G., Beck, P., Bernard, S., Bernardi, P.,
671 Bernt, M. H., Berrocal, A., Beyssac, O., Caïs, P., Castro, C., Castro, K., Clegg, S. M., Cloutis, E.,
672 Dromart, G., Drouet, C., Dubois, B., Escribano, D., Fabre, C., Fernandez, A., Forni, O., Garcia-
673 Baonza, V., Gontijo, I., Johnson, J., Laserna, J., Lasue, J., Madsen, S., Mateo-Marti, E., Medina,
674 J., Meslin, P.-Y., Montagnac, G., Moral, A., Moros, J., Ollila, A. M., Ortega, C., Prieto-Ballesteros,
675 O., Reess, J. M., Robinson, S., Rodriguez, J., Saiz, J., Sanz-Arranz, J. A., Sard, I., Sautter, V.,
676 Sobron, P., Toplis, M., and Veneranda, M. (2020). SuperCam Calibration Targets: Design and
677 Development. *Space Science Reviews*, 216(8):138.

678 Maurice, S. A. and Wiens, R. C. (2021). Mars 2020 SuperCam Bundle.

679 McMahon, S., Bosak, T., Grotzinger, J. P., Milliken, R. E., Summons, R. E., Daye, M., Newman,
680 S. A., Fraeman, A., Williford, K. H., and Briggs, D. E. G. (2018). A Field Guide to Finding Fossils
681 on Mars. *Journal of Geophysical Research (Planets)*, 123:1012–1040.

682 Megevand, V., Viennet, J., Balan, E., Gauthier, M., Rosier, P., Morand, M., Garino, Y., Guillaumet,
683 M., Pont, S., Beyssac, O., and Bernard, S. (2021). Impact of UV Radiation on the Raman Signal
684 of Cystine: Implications for the Detection of S-rich Organics on Mars. *Astrobiology*, 21(5):566–574.

685 Meyer, M. A., Kminek, G., Beaty, D. W., Carrier, B. L., Haltigin, T., Hays, L. E., Agree, C. B.,
686 Busemann, H., Cavalazzi, B., Cockell, C. S., Debaille, V., Glavin, D. P., Grady, M. M., Hauber,
687 E., Hutzler, A., Marty, B., McCubbin, F. M., Pratt, L. M., Regberg, A. B., Smith, A. L., Smith,
688 C. L., Summons, R. E., Swindle, T. D., Tait, K. T., Tosca, N. J., Udry, A., Usui, T., Velbel, M. A.,
689 Wadhwa, M., Westall, F., and Zorzano, M.-P. (2022). Final Report of the Mars Sample Return
690 Science Planning Group 2 (MSPG2). *Astrobiology*, 22(S1):S–5.

691 Meza, O., Villabona-Leal, E. G., Diaz-Torres, L. A., Desirena, H., Rodríguez-López, J. L., and Pérez,
692 E. (2014). Luminescence Concentration Quenching Mechanism in Gd2O3:Eu3+. *The Journal of*
693 *Physical Chemistry A*, 118(8):1390–1396.

694 Moeller, R. C., Jandura, L., Rosette, K., Robinson, M., Samuels, J., Silverman, M., Brown, K., Duffy,
695 E., Yazzie, A., Jens, E., Brockie, I., White, L., Goreva, Y., Zorn, T., Okon, A., Lin, J., Frost,
696 M., Collins, C., Williams, J. B., Steltzner, A., Chen, F., and Biesiadecki, J. (2020). The Sampling

and Caching Subsystem (SCS) for the Scientific Exploration of Jezero Crater by the Mars 2020 Perseverance Rover. *Space Science Reviews*, 217(1):5.

Morris, R. V. and Lauer, H. V. (1980). The case against UV photostimulated oxidation of magnetite. *Geophysical Research Letters*, 7(8):605–608.

Mukhin, L. M., Koscheevi, A. P., Dikov, Yu. P., Huth, J., and Wänke, H. (1996). Experimental simulations of the photodecomposition of carbonates and sulphates on Mars. *Nature*, 379:141–143.

Murchie, S. L., Mustard, J. F., Ehlmann, B. L., Milliken, R. E., Bishop, J. L., McKeown, N. K., Dobrea, E. Z. N., Seelos, F. P., Buczkowski, D. L., Wiseman, S. M., Arvidson, R. E., Wray, J. J., Swayze, G., Clark, R. N., Marais, D. J. D., McEwen, A. S., and Bibring, J.-P. (2009). A synthesis of Martian aqueous mineralogy after 1 Mars year of observations from the Mars Reconnaissance Orbiter. *Journal of Geophysical Research: Planets*, 114(E2).

Mustard, J. F., Murchie, S. L., Pelkey, S. M., Ehlmann, B. L., Milliken, R. E., Grant, J. A., Bibring, J.-P., Poulet, F., Bishop, J., Dobrea, E. N., Roach, L., Seelos, F., Arvidson, R. E., Wiseman, S., Green, R., Hash, C., Humm, D., Malaret, E., McGovern, J. A., Seelos, K., Clancy, T., Clark, R., Marais, D. D., Izenberg, N., Knudson, A., Langevin, Y., Martin, T., McGuire, P., Morris, R., Robinson, M., Roush, T., Smith, M., Swayze, G., Taylor, H., Titus, T., and Wolff, M. (2008). Hydrated silicate minerals on Mars observed by the Mars Reconnaissance Orbiter CRISM instrument. *Nature*, 454(7202):305–309.

Patel, M. R., Zarnecki, J. C., and Catling, D. C. (2002). Ultraviolet radiation on the surface of Mars and the Beagle 2 UV sensor. *Planetary and Space Science*, 50(9):915–927.

Poch, O., Kaci, S., Stalport, F., Szopa, C., and Coll, P. (2014). Laboratory insights into the chemical and kinetic evolution of several organic molecules under simulated Mars surface UV radiation conditions. *Icarus*, 242:50–63.

Poch, O., Noblet, A., Stalport, F., Correia, J. J., Grand, N., Szopa, C., and Coll, P. (2013). Chemical evolution of organic molecules under Mars-like UV radiation conditions simulated in the laboratory with the "Mars organic molecule irradiation and evolution" (MOMIE) setup. *Planetary and Space Science*, 85:188–197.

Poitras, J. T., Cloutis, E. A., Salvatore, M. R., Mertzman, S. A., Applin, D. M., and Mann, P. (2018). Mars analog minerals' spectral reflectance characteristics under Martian surface conditions. *Icarus*, 306:50–73.

Pollack, J. B., Roush, T., Witteborn, F., Bregman, J., Wooden, D., Stoker, C., and Toon, O. B. (1990). Thermal emission spectra of Mars (5.4-10.5 microns) - Evidence for sulfates, carbonates, and hydrates. *Journal of Geophysical Research*, 95:14595–14627.

Poulet, F., Bibring, J.-P., Mustard, J. F., Gendrin, A., Mangold, N., Langevin, Y., Arvidson, R. E., Gondet, B., and Gomez, C. (2005). Phyllosilicates on Mars and implications for early martian climate. *Nature*, 438(7068):623–627.

Rapin, W., Meslin, P. Y., Maurice, S., Vaniman, D., Nachon, M., Mangold, N., Schröder, S., Gasnault, O., Forni, O., Wiens, R. C., Martínez, G. M., Cousin, A., Sautter, V., Lasue, J., Rampe, E. B., and Archer, D. (2016). Hydration state of calcium sulfates in Gale crater, Mars: Identification of bassanite veins. *Earth and Planetary Science Letters*, 452:197–205.

Rull, F., Maurice, S., Hutchinson, I., Moral, A., Perez, C., Diaz, C., Colombo, M., Belenguer, T., Lopez-Reyes, G., Sansano, A., Forni, O., Parot, Y., Striebig, N., Woodward, S., Howe, C., Tarcea, N., Rodriguez, P., Seoane, L., Santiago, A., Rodriguez-Prieto, J. A., Medina, J., Gallego, P., Canchal, R., Santamaría, P., Ramos, G., Vago, J. L., and RLS Team (2017). The Raman Laser Spectrometer for the ExoMars Rover Mission to Mars. *Astrobiology*, 17:627–654.

Scheller, E. L., Razzell Hollis, J., Cardarelli, E. L., Steele, A., Beegle, L. W., Bhartia, R., Conrad, P., Uckert, K., Sharma, S., Ehlmann, B. L., Abbey, W. J., Asher, S. A., Benison, K. C., Berger, E. L., Beyssac, O., Bleefeld, B. L., Bosak, T., Brown, A. J., Burton, A. S., Bykov, S. V., Cloutis, E., Fairén, A. G., DeFlores, L., Farley, K. A., Fey, D. M., Fornaro, T., Fox, A. C., Fries, M., Hickman-Lewis, K., Hug, W. F., Huggett, J. E., Imbeah, S., Jakubek, R. S., Kah, L. C., Kelemen, P., Kennedy, M. R., Kizovski, T., Lee, C., Liu, Y., Mandon, L., McCubbin, F. M., Moore, K. R., Nixon, B. E., Núñez, J. I., Rodriguez Sanchez-Vahamonde, C., Roppel, R. D., Schulte, M., Sephton, M. A., Sharma, S. K., Siljeström, S., Shkolyar, S., Shuster, D. L., Simon, J. I., Smith, R. J., Stack, K. M., Steadman, K., Weiss, B. P., Werynski, A., Williams, A. J., Wiens, R. C., Williford, K. H., Winchell, K., Wogsland,

751 B., Yanchilina, A., Yingling, R., and Zorzano, M.-P. (2022a). Aqueous alteration processes in Jezero
752 crater, Mars—implications for organic geochemistry. *Science*, 378:1105–1110.

753 Scheller, E. L., Razzell Hollis, J., Cardarelli, E. L., Steele, A., Beegle, L. W., Bhartia, R., Conrad,
754 P., Uckert, K., Sharma, S., Ehlmann, B. L., Asher, S., Berger, E. L., Burton, A. S., Bykov, S.,
755 Fornaro, T., Fox, A. C., Fries, M., Kah, L. C., Kizovski, T., McCubbin, F. M., Moore, K., Roppel,
756 R., Shkolyar, S. O., Siljeström, S., Williams, A. J., Wogsland, B., and Wiens, R. C. (2022b).
757 First-Results from the Perseverance SHERLOC Investigation: Aqueous Alteration Processes and
758 Implications for Organic Geochemistry in Jezero Crater, Mars. *53rd Lunar and Planetary Science*
759 *Conference*, 2678:1652.

760 Squyres, S. W., Arvidson, R. E., Bell, J. F., Brückner, J., Cabrol, N. A., Calvin, W., Carr, M. H.,
761 Christensen, P. R., Clark, B. C., Crumpler, L., Marais, D. J. D., d'Uston, C., Economou, T., Farmer,
762 J., Farrand, W., Folkner, W., Golombek, M., Gorevan, S., Grant, J. A., Greeley, R., Grotzinger,
763 J., Haskin, L., Herkenhoff, K. E., Hviid, S., Johnson, J., Klingelhöfer, G., Knoll, A. H., Landis,
764 G., Lemmon, M., Li, R., Madsen, M. B., Malin, M. C., McLennan, S. M., McSween, H. Y., Ming,
765 D. W., Moersch, J., Morris, R. V., Parker, T., Rice, J. W., Richter, L., Rieder, R., Sims, M.,
766 Smith, M., Smith, P., Soderblom, L. A., Sullivan, R., Wänke, H., Wdowiak, T., Wolff, M., and Yen,
767 A. (2004a). The Opportunity Rover's Athena Science Investigation at Meridiani Planum, Mars.
768 *Science*, 306(5702):1698–1703.

769 Squyres, S. W., Grotzinger, J. P., Arvidson, R. E., Bell, J. F., Calvin, W., Christensen, P. R., Clark,
770 B. C., Crisp, J. A., Farrand, W. H., Herkenhoff, K. E., Johnson, J. R., Klingelhöfer, G., Knoll,
771 A. H., McLennan, S. M., McSween, H. Y., Morris, R. V., Rice, J. W., Rieder, R., and Soderblom,
772 L. A. (2004b). In Situ Evidence for an Ancient Aqueous Environment at Meridiani Planum, Mars.
773 *Science*, 306(5702):1709–1714.

774 Stalport, F., Coll, P., Szopa, C., Cottin, H., and Raulin, F. (2009). Investigating the Photostability of
775 Carboxylic Acids Exposed to Mars Surface Ultraviolet Radiation Conditions. *Astrobiology*, 9(6):543–
776 549.

777 Stalport, F., Rouquette, L., Poch, O., Dequaire, T., Chaouche-Mechidal, N., Payart, S., Szopa, C.,
778 Coll, P., Chaput, D., Jaber, M., Raulin, F., and Cottin, H. (2019). The Photochemistry on Space

779 Station (PSS) Experiment: Organic Matter under Mars-like Surface UV Radiation Conditions in
780 Low Earth Orbit. *Astrobiology*, 19:1037–1052.

781 ten Kate, I. L., Garry, J. R. C., Peeters, Z., Foing, B., and Ehrenfreund, P. (2006). The effects of
782 Martian near surface conditions on the photochemistry of amino acids. *Planetary and Space Science*,
783 54(3):296–302.

784 Turenne, N., Parkinson, A., Applin, D. M., Mann, P., Cloutis, E. A., and Mertzman, S. A. (2022).
785 Spectral reflectance properties of minerals exposed to martian surface conditions: Implications for
786 spectroscopy-based mineral detection on Mars. *Planetary and Space Science*, 210:105377.

787 Vaniman, D. T., Bish, D. L., Chipera, S. J., Fialips, C. I., William Carey, J., and Feldman, W. C.
788 (2004). Magnesium sulphate salts and the history of water on Mars. *Nature*, 431:663–665.

789 Viennet, J.-C., Bultel, B., and Werner, S. C. (2019). Experimental reproduction of the martian
790 weathering profiles argues for a dense Noachian CO2 atmosphere. *Chemical Geology*, 525:82–95.

791 Wang, A., Freeman, J. J., Jolliff, B. L., and Chou, I.-M. (2006). Sulfates on Mars: A systematic Raman
792 spectroscopic study of hydration states of magnesium sulfates. *Geochimica et Cosmochimica Acta*,
793 70(24):6118–6135.

794 Wiens, R. C., Maurice, S., Robinson, S. H., Nelson, A. E., Cais, P., Bernardi, P., Newell, R. T., Clegg,
795 S., Sharma, S. K., Storms, S., Deming, J., Beckman, D., Ollila, A. M., Gasnault, O., Anderson,
796 R. B., André, Y., Michael Angel, S., Arana, G., Auden, E., Beck, P., Becker, J., Benzerara, K.,
797 Bernard, S., Beyssac, O., Borges, L., Bousquet, B., Boyd, K., Caffrey, M., Carlson, J., Castro,
798 K., Celis, J., Chide, B., Clark, K., Cloutis, E., Cordoba, E. C., Cousin, A., Dale, M., Deflores, L.,
799 Delapp, D., Deleuze, M., Dirmyer, M., Donny, C., Dromart, G., George Duran, M., Egan, M., Ervin,
800 J., Fabre, C., Fau, A., Fischer, W., Forni, O., Fouchet, T., Fresquez, R., Frydenvang, J., Gasway,
801 D., Gontijo, I., Grotzinger, J., Jacob, X., Jacquinod, S., Johnson, J. R., Klisiewicz, R. A., Lake, J.,
802 Lanza, N., Laserna, J., Lasue, J., Le Mouélic, S., Legett, C., Leveille, R., Lewin, E., Lopez-Reyes,
803 G., Lorenz, R., Lorigny, E., Love, S. P., Lucero, B., Madariaga, J. M., Madsen, M., Madsen, S.,
804 Mangold, N., Manrique, J. A., Martinez, J. P., Martinez-Frias, J., McCabe, K. P., McConnochie,
805 T. H., McGlown, J. M., McLennan, S. M., Melikechi, N., Meslin, P.-Y., Michel, J. M., Mimoun,
806 D., Misra, A., Montagnac, G., Montmessin, F., Mousset, V., Murdoch, N., Newsom, H., Ott, L. A.,

807 Ousnamer, Z. R., Pares, L., Parot, Y., Pawluczyk, R., Glen Peterson, C., Pilleri, P., Pinet, P.,
808 Pont, G., Poulet, F., Provost, C., Quertier, B., Quinn, H., Rapin, W., Reess, J.-M., Regan, A. H.,
809 Reyes-Newell, A. L., Romano, P. J., Royer, C., Rull, F., Sandoval, B., Sarrao, J. H., Sautter, V.,
810 Schoppers, M. J., Schröder, S., Seitz, D., Shepherd, T., Sobron, P., Dubois, B., Sridhar, V., Toplis,
811 M. J., Torre-Fdez, I., Trettel, I. A., Underwood, M., Valdez, A., Valdez, J., Venhaus, D., and
812 Willis, P. (2021). The SuperCam Instrument Suite on the NASA Mars 2020 Rover: Body Unit and
813 Combined System Tests. *Space Science Reviews*, 217(1):4.

814 Wiens, R. C., Udry, A., Beyssac, O., Quantin-Nataf, C., Mangold, N., Cousin, A., Mandon, L., Bosak,
815 T., Forni, O., McLennan, S. M., Sautter, V., Brown, A., Benzerara, K., Johnson, J. R., Mayhew,
816 L., Maurice, S., Anderson, R. B., Clegg, S. M., Crumpler, L., Gabriel, T. S. J., Gasda, P., Hall, J.,
817 Horgan, B. H. N., Kah, L., Legett, C., Madariaga, J. M., Meslin, P.-Y., Ollila, A. M., Poulet, F.,
818 Royer, C., Sharma, S. K., Siljeström, S., Simon, J. I., Acosta-Maeda, T. E., Alvarez-Llamas, C.,
819 Angel, S. M., Arana, G., Beck, P., Bernard, S., Bertrand, T., Bousquet, B., Castro, K., Chide, B.,
820 Clavé, E., Cloutis, E., Connell, S., Dehouck, E., Dromart, G., Fischer, W., Fouchet, T., Francis,
821 R., Frydenvang, J., Gasnault, O., Gibbons, E., Gupta, S., Hausrath, E. M., Jacob, X., Kalucha, H.,
822 Kelly, E., Knutsen, E., Lanza, N., Laserna, J., Lasue, J., Le Mouélic, S., Leveille, R., Lopez Reyes,
823 G., Lorenz, R., Manrique, J. A., Martinez-Frias, J., McConnochie, T., Melikechi, N., Mimoun,
824 D., Montmessin, F., Moros, J., Murdoch, N., Pilleri, P., Pilorget, C., Pinet, P., Rapin, W., Rull,
825 F., Schröder, S., Shuster, D. L., Smith, R. J., Stott, A. E., Tarnas, J., Turenne, N., Veneranda,
826 M., Vogt, D. S., Weiss, B. P., Willis, P., Stack, K. M., Williford, K. H., Farley, K. A., and THE
827 SUPERCAM TEAM (2022). Compositionally and density stratified igneous terrain in Jezero crater,
828 Mars. *Science Advances*, 8(34):eabo3399.

829 Yen, A. S., Murray, B., Rossman, G. R., and Grunthaner, F. J. (1999). Stability of hydroxylated
830 minerals on Mars: A study on the effects of exposure to ultraviolet radiation. *Journal of Geophysical*
831 *Research: Planets*, 104(E11):27031–27041.